

**DESIGN AND CONTROL OF COOLING RATE FOR IMPROVING
THE STRENGTH OF GRAY CAST IRONS**

KITTIKHUN SEAWSAKUL

**A THESIS SUBMITTED IN PARTIAL FULFILLMENT OF THE REQUIREMENTS
FOR THE DEGREE OF MASTER OF SCIENCE
MAJOR IN PHYSICS FACULTY OF SCIENCE
UBON RATCHATHANI UNIVERSITY
YEAR 2013
COPYRIGHT OF UBON RATCHATHANI UNIVERSITY**



UBON RATCHATHANI UNIVERSITY
THESIS APPROVAL
MASTER OF SCIENCE
MAJOR IN PHYSICS FACULTY OF SCIENCE

TITLE DESIGN AND CONTROL OF COOLING RATE FOR IMPROVING
THE STRENGTH OF GRAY CAST IRONS

AUTHOR MR. KITTIKHUN SEAWSAKUL

EXAMINATION COMMITTEE

ASST. PROF. DR. TANIN NUTARO	CHAIRPERSON
ASST. PROF. DR. UDOM TIPPARACH	MEMBER
DR. CHRISTIAN HERBST	MEMBER
DR. TIPPAWAN SAIPIN	MEMBER

ADVISOR

Ud. Tipparach

(ASST. PROF. DR. UDOM TIPPARACH)

Utith Inprasit

(ASSOC. PROF. DR. UTITH INPRASIT)

DEAN, FACULTY OF SCIENCE

H. Juthamas

(DR. JUTHAMAS HONGTHONG)

ACTING FOR VICE PRESIDENT

FOR ACADEMIC AFFAIRS

COPYRIGHT OF UBON RATCHATHANI UNIVERSITY

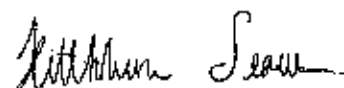
ACADEMIC YEAR 2013

ACKNOWLEDGEMENTS

I thank my advisor, Asst. Prof. Dr.Udom Tipparach, who have helped me in many respects, encouraged, guided and supported from the initial to the final level that enable me to develop understanding physical and real worlds. Special thanks the also to Asst. Prof. Suriya Choksawadee and Dr.Charuayporn Santhaweesuk, Department of Industrial Engineering, Ubon Ratchathani University for valuable advices, sample preparation and helpful suggestions.

I am indebted to Dr.Greg Heness, Department of Physics and Advanced Materials, University of Technology Sydney, Australia, who gave useful suggestion, taught about sample preparation and characterization, and provided valuable information. I appreciate the thesis committee; Asst Prof. Dr.Tanin mutaro and Dr. Christian Herbst for their kindly advices and helpful suggestions. I would like to thank the external committee member, Dr. Tippawan Saipin from Ubon Ratchathani Technical College for her comments and suggestions. In addition, I am grateful all faculty members and staff in Department of Physics, Faculty of Science and Department of Industrial Engineering, Ubon Ratchathani University for their teaching and technical supports for this work.

Most of all, I thank my beloved family for their encouragement supports and nourishment that found me to be a fortitude person.



(MR. Kittikhun Seawsakul)

Researcher

บทคัดย่อ

ชื่อเรื่อง : การออกแบบและควบคุมอัตราการใช้พลังงานเพื่อเพิ่มคุณสมบัติความต้านทานแรงดึง
ของเหล็กหล่อเทา

โดย : กิตติคุณ เขียวสกุล

ชื่อปริญญา : วิทยาศาสตร์มหาบัณฑิต

สาขาวิชา : ฟิสิกส์

ประธานกรรมการที่ปรึกษา : ผู้ช่วยศาสตราจารย์ ดร.อุดม ทิพราช

คำสำคัญ : อัตราการใช้พลังงาน ความต้านทานแรงดึง เหล็กหล่อเทา การเลี้ยวเบนของรังสีเอกซ์

การควบคุมอัตราการใช้พลังงานของเหล็กหล่อเทาในขณะที่ทำการหล่อสามารถช่วยเพิ่มคุณภาพของเหล็กหล่อเทา เราได้ทำการตรวจสอบ โครงสร้างและคุณสมบัติของเหล็กหล่อเทาที่ได้รับจากการควบคุมจากอัตราการใช้พลังงานในแบบหล่อที่มีขนาดความหนาของแบบหล่อที่แตกต่างกัน ขึ้นตัวอย่างของเหล็กหล่อเทาได้ถูกทำโดยการควบคุมอัตราการใช้พลังงานในขณะที่น้ำเหล็กเริ่มเปลี่ยนสถานะกลายเป็นของแข็ง แบบหล่อถูกทำขึ้นมาจากทรายและมีลักษณะเป็นทรงกระบอก กระบวนการของการถ่ายโอนความร้อนของเหล็กได้ถูกเก็บข้อมูล โดยมีอัตราการใช้พลังงานตามแนวรัศมีของความหนาของแบบหล่อ เทคนิคของการเลี้ยวเบนของรังสีเอกซ์ได้ถูกนำมาใช้ในการระบุโครงสร้างเฟสและกล้องจุลทรรศน์แสงได้ถูกนำมาใช้ในการศึกษาโครงสร้างจุลภาค เครื่อง Optical emission spectroscopy ได้ถูกนำมาใช้ในการตรวจสอบองค์ประกอบของธาตุที่เป็นองค์ประกอบของเหล็กหล่อเทา เหล็กหล่อเทาที่ผลิตทั้งสามแบบมีความหนาตามแนวรัศมีเป็น 0.7, 1.5 และ 2.8 นิ้ว ได้ถูกหล่อและถูกทดสอบค่าความต้านทานแรงดึง ผลการทดสอบแสดงให้เห็นว่า ค่าความต้านทานแรงดึงของเหล็กหล่อเทาที่หล่อด้วยแบบหล่อทรายผนังหนา 1.5 นิ้ว มีค่าความต้านทานแรงดึงที่ดีที่สุด

ABSTRACT

TITLE : DESIGN AND CONTROL OF COOLING RATE FOR IMPROVING
THE STRENGTH OF GRAY CAST IRONS

BY : KITTIKHUN SEAWSAKUL

DEGREE : MASTER OF SCIENCE

MAJOR : PHYSICS

CHAIR : ASST.PROF.UDOM TIPPARACH, Ph.D.

KEYWORDS : COOLING RATE / TENSILE STRENGTH / GRAY CAST IRON / X-RAY
DIFFRACTION

The quality of gray cast iron was enhanced by controlling the cooling rate of cast iron in the manufacturing process. We have investigated the structures and properties of the gray cast irons obtained the control of the cooling rate with different mold wall thickness. The cast iron specimens were made by controlling the cooling rate in the solidification process. The mold was cylindrical in shape and made of sand. The process of the heat transfer of the materials was investigated. The heat transfer rate was considered as the radial thickness of the mold wall. The X-ray diffraction (XRD) technique was used to identify the phase and optical microscope used to study the microstructure. Optical emission spectroscopy was employed to examine the constituent of the specimens. Three gray cast irons with the mold wall thickness of 0.7, 1.5, and 2.8 inches, respectively, were casted and tested for tensile strength. The results showed that the specimens made of 1.5 inch radial mold thickness yielded the highest tensile strength.

CONTENTS

	PAGE
ACKNOWLEDGMENTS	I
THAI ABSTRACT	II
ENGLISH ABSTRACT	III
CONTENTS	IV
LIST OF TABLES	VI
LIST OF FIGURES	VII
CHAPTER	
1 INTRODUCTION	
1.1 Motivation and background	1
1.2 Gray cast iron	3
1.3 Mechanical properties of gray cast iron	5
1.4 Research objectives	6
2 THEORETICAL AND LITERATURE REVIEWS	
2.1 Metallic Crystal Structures	7
2.2 The metallic bond	8
2.3 Solidification	9
2.4 Graphite	13
2.5 Chemical composition	17
2.6 The induction furnace	18
2.7 Mechanical properties of gray cast iron	19
2.7.1 The importance of cooling rate and section sensitivity	20
2.7.2 Hardness and its relationship with tensile strength	21
2.8 Heat transfer and solidification	21
3 EXPERIMENTAL	
3.1 The casting process	25
3.1.1 Composition of gray cast iron	25

CONTENTS (CONTINUED)

	PAGE
3.1.2 Induction furnace practice	26
3.1.3 Mold preparation	27
3.1.4 Thermocouple	29
3.2 Process of mechanical preparation	30
3.2.1 Tensile strength	30
3.2.2 Percentage elongation	30
3.3.3 The Rockwell test	32
3.3.4 The heat transfer	32
3.3 Emission Spectrometer	33
3.4 Preparation of metallography and microstructures	34
3.4.1 Microstructure	34
3.4.2 Scanning Electron Microscopy (SEM)	36
3.4.3 X-ray Diffraction Analysis (XRD)	39
 4 RESULTS AND DISCUSSION	
4.1 Mechanical property	38
4.2 Emission spectrochemical analysis	39
4.3 Metallography and Microstructures	40
4.4 Scanning electron microscopy analysis	43
4.5 X-ray diffraction patterns	47
 5 CONCLUSIONS AND SUGGESTION	 48
 REFERENCES	 50
 APPENDIX	 55
 VITAE	 67

LIST OF TABLES

TABLES	PAGE
1.1 Types of Cast Iron	4
2.1 Summary of factors affecting slip in metallic structures	8
2.2 Constituents commonly found in cast iron microstructures, and their general effect on physical properties	12
3.1 Chemical composition (in wt%) of gray cast iron	25
3.2 Chemical compounds of inoculants	25
4.1 The average of the mechanical testing	38
4.2 Chemical compositions of the gray cast iron	40

LIST OF FIGURES

FIGURES	PAGE
1.1 Shows a metal that has two constituents	2
1.2 Classification scheme for the various ferrous alloys	3
1.3 Gray iron: the dark graphite flakes are embedded in a ferrite matrix	4
1.4 The stress and strain curve	5
1.5 Rockwell hardness tester	6
2.1 Principal metal crystal structure	7
2.2 (a) Bonding and (b) anti-bonding molecular orbitals of the H_2^+ molecule. (c) Schematic drawing of the building of the most important molecular orbitals from atomic orbitals and (d), (e) examples of molecular orbitals (bonding: σ , π and anti-bonding σ^* , π^*)	9
2.3 Modified iron-carbon equilibrium or phase diagram	11
2.4 Reference diagram for the distribution of graphite	13
2.5 ASTM A-247 provides also a standard for evaluating the size of graphite. A chart shows standard graphite size from one to eight for one hundred	15
2.6 The difference in electrode potentials between the ferrite/iron carbide matrix and the graphite flakes is very large. This results in mini-galvanic cells with graphite as the cathode and the ferrite/iron carbide matrix as the sacrificial anode, which is the primary cause of the very poor corrosion resistance of gray cast iron	16
2.7 Crucibles may also be equipped with strong lids to lessen how much air has access to the melting metal until it is poured out, making a purer melt	19
2.8 Approximate relationship between tensile strength and Brinell Hardness of irons produced in one foundry	21

LIST OF FIGURES (CONTINUED)

FIGURES	PAGE
2.9 Thermal conditions for solidification of a simple geometry of a pure superheated liquid metal. In the figure, K corresponds to heat transfer by conduction, N to Newtonian heat transfer across the mould-metal interface, C to convective heat transfer, and R to heat transfer by radiation	22
2.10 Schematic illustration of primary spacing adjustment mechanism for dendrites	23
3.1 (a) The iron Scrap, and (b) Inoculants	26
3.2 Starting the pouring process for the melted iron	27
3.3 River sand mixture with bentonite clay and water	28
3.4 The wall thickness of 0.7, 1.5, and 2.8 inches	28
3.5 Diagram of casting process	29
3.6 Dimensions of the tension test specimen	30
3.7 (a) Gray cast iron from the casting process, (b) It has been turning by a CNC machine, (c) Testing tensile strength and Percentage elongation	31
3.8 The steps in measurement of hardness with a sphere of steel and showed Rockwell scale hardness tester model: AR-10	32
3.9 ARL 3460 Fisons Instruments	33
3.10 (a) The samples before testing and (b) after testing	34
3.11 (a)The samples of polishing surface and (b) Use of rotating wheel polisher	34
3.12 Etching by Nital in Chemical Fume Hood	35
3.13 The microscopes to connect with computer	35
3.14 Diagram of Metallurgical specimen preparation	36
3.15 Direction of polishing on a rotating wheel	36
3.16 A JEOL JSM-5410 Scanning Electron Microscopy	37
3.17 A PHILIPS X'Pert MPD diffractometer	37
4.1 The plots of the cooling rate curves of the different mold wall thickness obtained	39

LIST OF FIGURES (CONTINUED)

FIGURES	PAGE
4.2 Microstructure of solidified gray cast iron from the mold wall thickness 0.7 inch	41
4.3 Microstructure of solidified gray cast iron from the mold wall thickness 1.5 inch	42
4.4 Microstructure of solidified gray cast iron from the mold wall thickness 2.8 inch	42
4.5 Tensile fracture surfaces of the mold wall thickness of 0.7 inches	44
4.6 Tensile fracture surfaces of the mold wall thickness of 1.5 inches	45
4.7 Tensile fracture surfaces of the mold wall thickness of 2.8 inches	46
4.8 XRD pattern of the gray cast iron specimen	47

CHAPTER 1

INTRODUCTION

1.1 Motivation and background

Gray cast iron has become a popular cast metal material which is widely applied in modern industrial manufactures due to its good castability, wear resistance, low melting point, machinability, high damping capacity and low cost. The microstructure of the gray cast iron is characterized by graphite flakes dispersed into the matrix [1].

Industrial casting practice can influence nucleation and the growth of graphite flakes, so that type and size increase the desired properties. The amount of the graphite and size, morphology and distribution of the graphite lamellas are essential in determining the mechanical quality of gray cast iron [2-3]. Thus, it is important to control the flake graphite morphology that has a direct influence on the properties of the gray cast iron. The structure of gray cast iron depends on chemical composition, inoculants, and cooling conditions [3]. The gray cast iron in general, is composed of the following material: carbon 2-4 percent, silicon 1-3 percent, manganese 1-1.5 percent, sulfur about 0.05 percent and phosphorus under 0.5 percent. The morphology of the graphite flakes can be modified by inoculating the iron melt to improve the fracture toughness or impact toughness and applying austempering heat treatments to improve the fracture toughness or impact toughness of monolithic gray cast iron [4-5]. The inoculation technique was an effective method to improve mechanical properties of gray cast iron parts [6].

In the case of gray cast iron, the graphite flakes are embedded in a metallic matrix, which may consist of any combination of five metallurgical constituents: Pearlite, Ferrite, Austenite, Cementite (Iron carbide), and Ledeburite. Since these micro-constituents have different properties. The metallurgical are apparent that if the form and relative amounts of the structure in the matrix can be controlled as desired and distribution can also be controlled, the cast iron is treated by controlling a cooling rate and constituents [7].

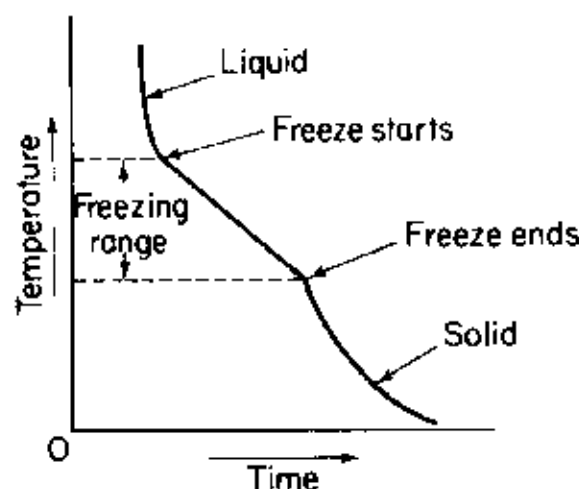


Figure 1.1 Shows a metal that has two constituents [9].

The cooling of the melt produces a curve somewhat like that of a pure metal. As the temperature at which freezing starts, the first solid that forms are richer in that constituent who has the higher freezing temperature (Figure 1.1). As the temperature at which the last freezing takes place, the metal was richer in that constituent which has a lower freezing point. The high cooling rates in producing fine structures results in increase of high-strength cast alloys. The undercooling of a melt to a lower temperature increases the number of effective nuclei relative to the growth rate and the final being restricted by the rate at which the latent heat of crystallization can be dissipated [9]. The refining influence of an enhanced cooling rate applies to grain size and to substructure [10].

Hence, this work presented the effect of cooling rate control with different sizes on the tensile strength, morphology, and microstructure of the specimens obtained from industrial castings made of gray cast iron, and produced by different radial thickness of the sand molds. The cooling rate was used to control the graphite flake morphology. Then, the mechanical properties of the gray cast iron were tested.

1.2 Gray cast iron

The metal alloys are often grouped into two classes; ferrous and nonferrous (Figure 1.2). The nonferrous metal is any metal, including alloys, that does not contain iron in appreciable amounts. Generally more expensive than ferrous metals, nonferrous metals are used because of desirable properties such as low weight, higher conductivity, non-magnetic property or resistance to corrosion. Some nonferrous materials are also used in the iron and steel industries. Ferrous alloys, those in which iron was the principal constituent, include the steels and the cast irons.

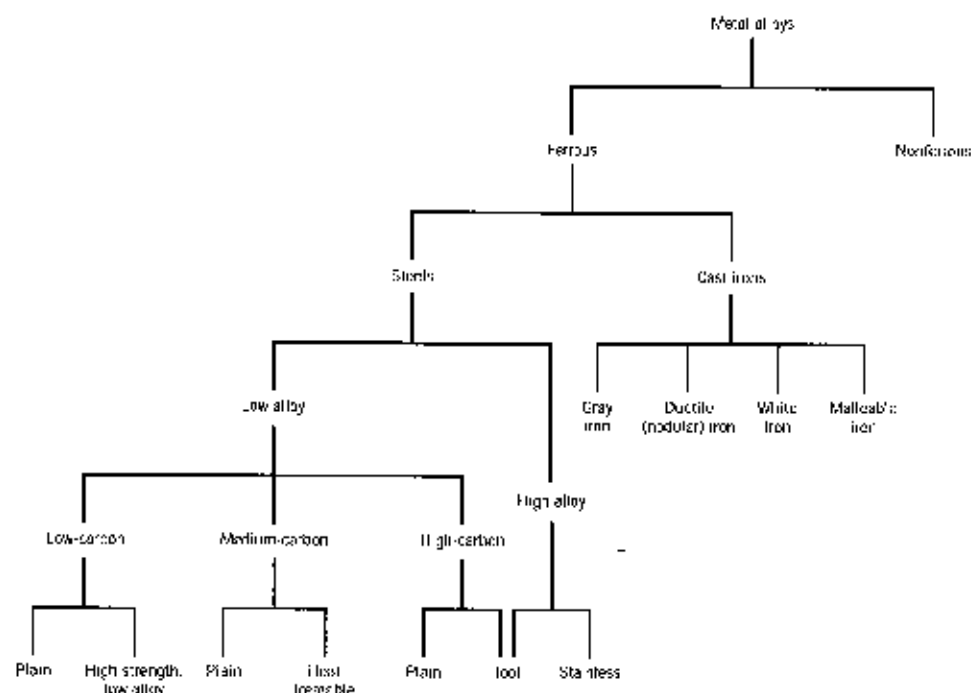


Figure 1.2 Classification scheme for the various ferrous alloys [11].

The cast irons are a class of ferrous alloys with carbon contents above 2.14 wt%, however, most cast irons contain between 3.0 and 4.5 wt% carbon. For most the cast irons, the carbon exists as graphite and both microstructure, and mechanical behavior depend on composition and heat treatment. The tendency to form graphite is regulated by the composition and rate of cooling. Graphite formation is promoted by the presence of silicon in concentrations greater than about 1 wt%. Also, slower cooling rates during solidification favor graphitization

(the formation of graphite). The most common cast iron types are Gray cast iron, Ductile Iron, Malleable cast iron and White cast iron.

Table 1.1 Types of Cast Iron.

Type of Iron	Carbon	Silicon	Manganese	Sulfur	Phosphorus
Gray cast iron	2.50 - 4.00	1.00 - 3.00	0.20 - 1.00	0.02 - 0.25	0.02 - 1.00
Ductile Iron	3.00 - 4.00	1.80 - 2.80	0.10 - 1.00	0.01 - 0.03	0.01 - 0.10
Malleable cast iron	2.00 - 2.90	0.90 - 1.90	0.15 - 1.20	0.02 - 0.20	0.02 - 0.20
White cast iron	1.80 - 3.60	0.50 - 1.90	0.25 - 0.80	0.06 - 0.20	0.06 - 0.20

The gray cast iron is a class of cast irons with carbon and silicon contents between 2.5 to 4.0 wt% and 1.0 to 3.0 wt%, respectively (Table 1.1). For most of these cast irons, the graphite exists in the form of flakes, which are normally surrounded by a ferrite or pearlite matrix. The microstructure of a typical gray cast iron, as shown in Figure 1.3. Because of these graphite flakes, a fractured surface takes on a gray color appearance, hence its name.

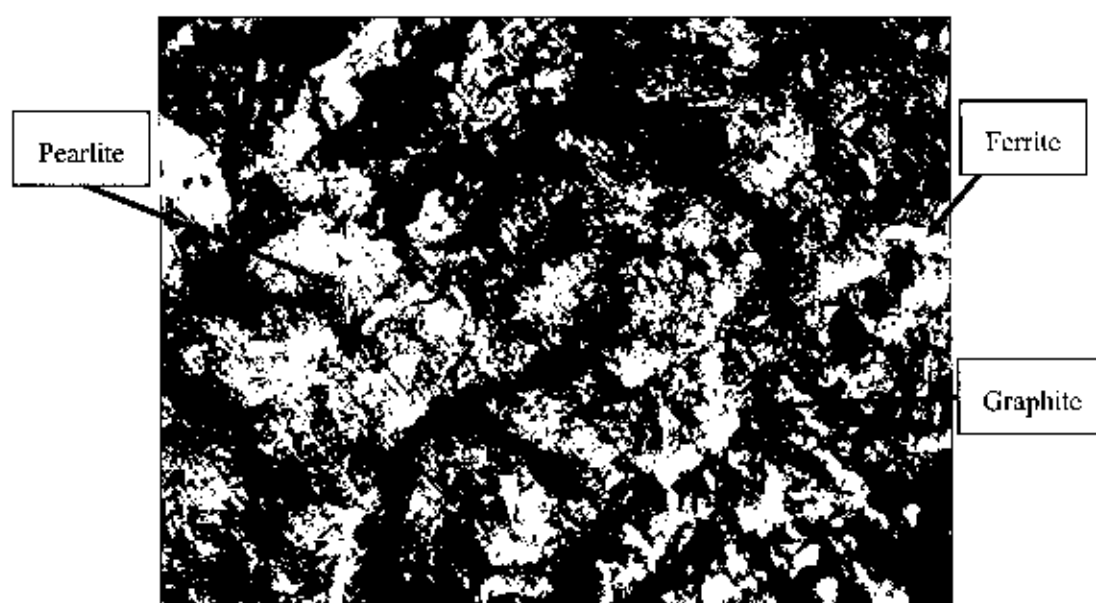


Figure 1.3 Gray iron: the dark graphite flakes are embedded in a ferrite matrix.

1.3 Mechanical properties of gray cast iron

The tensile strength measures the force required to pull something such as wood, iron, or a structural beam to the point where it breaks. By pulling on material, examiner will very quickly determine how the material will react to forces being applied in tension. As the material was being pulled, examiner will find its strength along with how much it will elongate. The tensile strength of a material was the maximum amount of tensile stress that it can take before failure, for example breaking. The tensile strength can be quoted as either true stress or engineering stress, but engineering stress was the most commonly used [12].

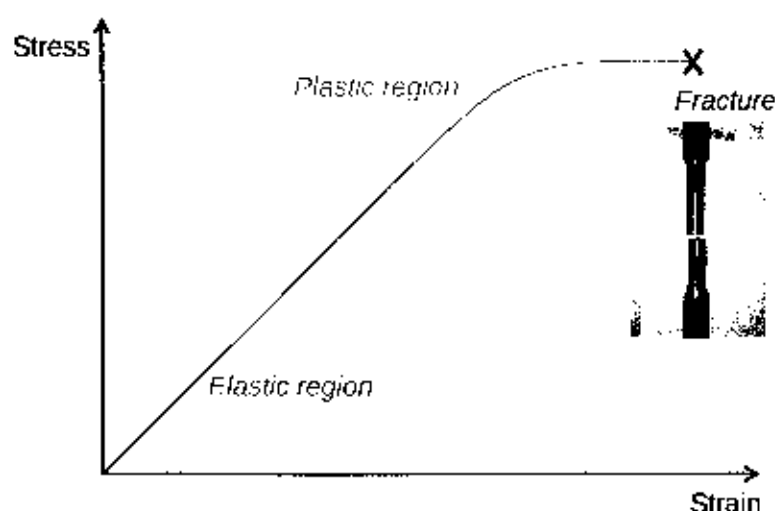


Figure 1.4 The stress and strain curve.

The hardness is the property of a material that enables it to resist plastic deformation. However, the term hardness may also refer to resistance to bending, scratching, abrasion or cutting. The usual method to achieve a hardness value is to measure the depth or area of an indentation left by an indenter of a specific shape, with a specific force applied for a specific time. There are four principal standard test methods for expressing the relationship between hardness and the size of the impression, these being Brinell, Vickers, Knoop and Rockwell.

The rockwell hardness test, this hardness test uses a direct reading instrument based on the principle of differential depth measurement. The test was carried out by slowly raising the specimen against the indenter until a fixed minor load has been applied (Figure 1.5). Then

the major load was applied through a loaded lever system. After the dial pointer comes to rest, the major load was removed and with the minor load still acting. The Rockwell hardness number was read on the dial gauge. Since the order of the numbers was reversed on the dial gauge, a shallow impression on a hard material will result in a high number while a deep impression on a soft material will result in a low number.



Figure 1.5 Rockwell hardness tester.

1.4 Research objectives

The objective of this work was to increase tensile strength of the gray cast iron. The tensile strength can be determined by the cooling rate of the mold. The cooling rate of the mold can be controlled by modifying the thickness of a sand mold to get the solidification process to improve the mechanical properties of gray cast iron. The measurement of the cooling rate was carried out using a digital multimeter equipped with a type K thermocouple. X-ray diffraction (XRD), optical microscope, and scanning electron microscopy (SEM) were used to characterize the gray cast iron. The tensile strength was measured and compared when different mold thickness were used in the manufacturing process.

CHAPTER 2

THEORETICAL AND LITERATURE REVIEWS

In this chapter, we review the theoretical background of gray cast iron structure and mechanical properties. We introduce heat transfer of casting process and related research works.

2.1 Metallic Crystal Structures

Most element metals (about 90 percent) crystallize upon solidification into three densely packed crystal structure: body-centered cubic (BCC), face-centered cubic (FCC), and hexagonal close-packed (HCP) [1]. Many of the common metals have either a body-centered cubic or face-centered cubic crystal structure [13]. It can be observed from binary phase diagrams that intermetallic compounds with a particular crystal structure are often accompanied by compounds with certain other crystal structures at other compositions [14]. Table 2.1 lists three important factors. That this discussion describes the behavior of nearly perfect single crystals. Most materials were seldom single crystals and always contain large numbers of defects. Since different crystals or grains are oriented in different random directions.

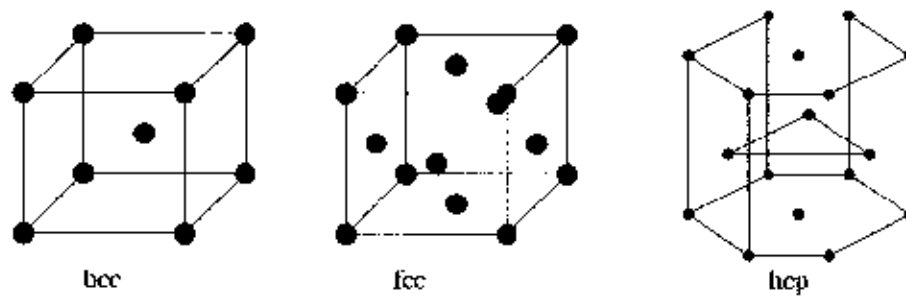


Figure 2.1 Principal metal crystal structure [1].

Table 2.1 Summary of factors affecting slip in metallic structures [15].

Factor	FCC	BCC	HCP
Critical resolved shear stress (psi)	50 – 100	5,000 – 10,000	50 – 100 ^a
Number of slip systems	12	48	3 ^b
Cross-slip	Can occur	Can occur	Cannot occur ^b
Summary of properties	Ductile	Strong	Relatively brittle

^a For slip on basal planes.

^b By alloying or heating to elevated temperatures, additional slip systems are active in HCP metals, permitting cross-slip to occur and thereby improving ductility.

2.2 The metallic bond

The metallic bond can be described in a similar way as the covalent bond. The main difference between these two bond types is that the ionization energy for electrons occupying the outer orbitals of the metallic elements is much smaller. In typical metals, like the alkali metals, these outer orbitals are spherical s-orbitals allowing overlapping with up to 12 further s-orbitals of the surrounding atoms. Thus, the well-defined electron localization in bonds connecting pairs of atoms with each other loses its meaning. Quantum-mechanical calculations show that in large agglomerations of metal atoms the delocalized bonding electrons occupy lower energy levels than in the free atoms; this would not be true for isolated “metal molecules”. The metallic bond in typical metals is non-directional, favoring structures corresponding to closest packing of spheres. With increasing localization of valence electrons, covalent interactions cause deviations from spherically symmetric bonding, leading to more complicated structures.

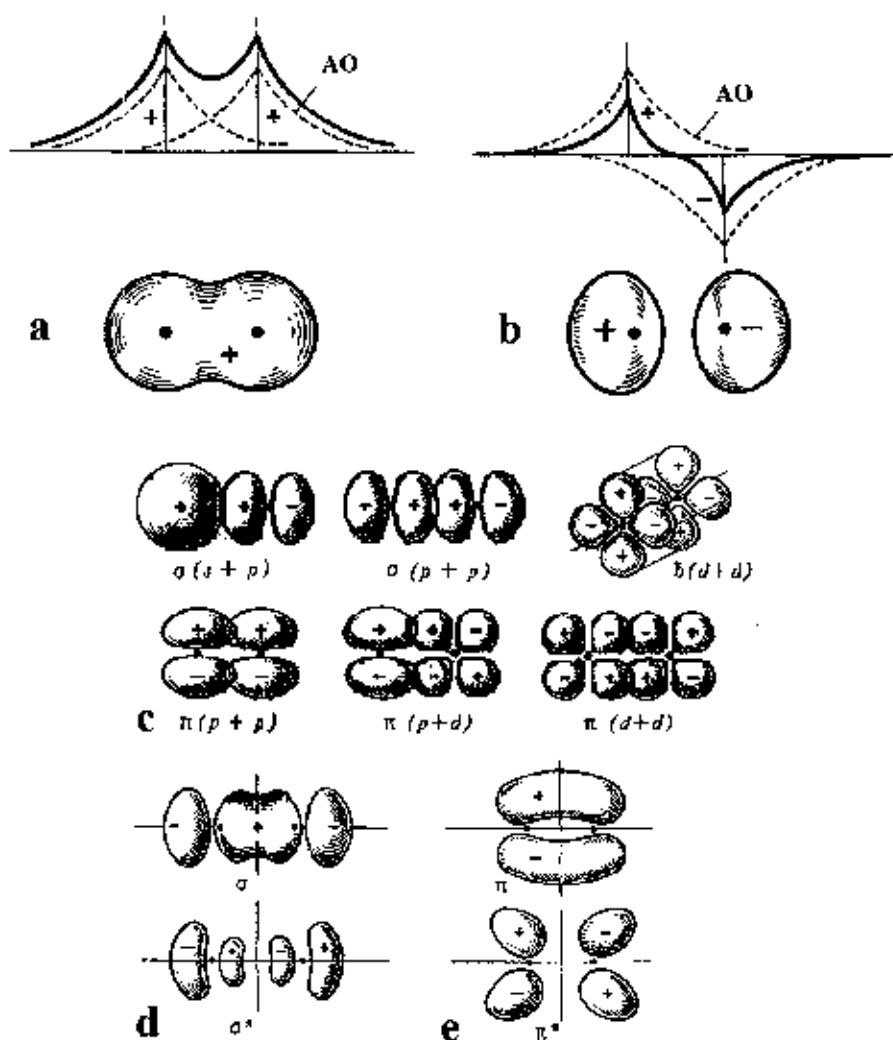


Figure 2.2 (a) Bonding and (b) anti-bonding molecular orbitals of the H_2 molecule.

(c) Schematic drawing of the building of the most important molecular orbitals from atomic orbitals and (d), (e) examples of molecular orbitals (bonding: σ , π and anti-bonding σ^* , π^*) [16].

2.3 Solidification

The structure and properties of the gray cast iron are largely determined by what happens during solidification and subsequent cooling. In the case of steel, the iron-carbon equilibrium diagram, as shown in Figure 2.3, can be used to interpret structure, under conditions of slow or near equilibrium transformation. The cast iron, however, may solidify either as the stable eutectic consisting of graphite, or as the metastable eutectic consisting of iron carbide

and austenite. Irons with graphite in the structure are termed gray cast irons, as on breaking the fracture occurs along the graphite and exhibits a gray fracture. When there is no graphite in the structure the iron breaks with a white fracture and is termed a 'white' or 'chilled' cast iron.

Chill effect: when molten metal contact the cold walls of a mould, the melt superheat is removed from the liquid and it becomes locally supercooled. The number of nucleation centers increase and nucleation takes place catastrophically in the liquid. Techniques such as splat cooling and die casting, as well as applications using chills employ this approach with varying efficiencies according to the sample size.

As shown in Figure 2.3, the eutectic of iron and carbon occurs with a carbon content of about 4.3 and melting point of 1130 °C. A binary eutectic consists of two solid phases produced by solidification at constant temperature. The eutectic alloy has the lowest freezing point in the system. Additions of silicon and phosphorus lower the percentage of carbon in the eutectic by about 0.33 percent for each 1 percent present. These effects can be incorporated into a formula which gives the carbon equivalent of the iron.

$$\text{Carbon equivalent (CE)} = \text{C}\% + \frac{(\text{Si}\% + \text{P}\%)}{3}$$

When the carbon equivalent is 4.3 the alloy is eutectic.

When less than 4.3 the gray cast iron is hypo-eutectic

When more than 4.3 the gray cast iron is hypereutectic.

The carbon equivalent value describes, therefore, how close a given analysis is to that of the eutectic composition. Thus, an iron with a total carbon content of 3.2 percent, silicon 2.0 percent and phosphorus 0.4 percent, has a CE value of 4.0 and is hypo-eutectic. As the carbon equivalent value decreases, the strength of a gray cast iron will increase-because less of the matrix will be interrupted by graphite [7].

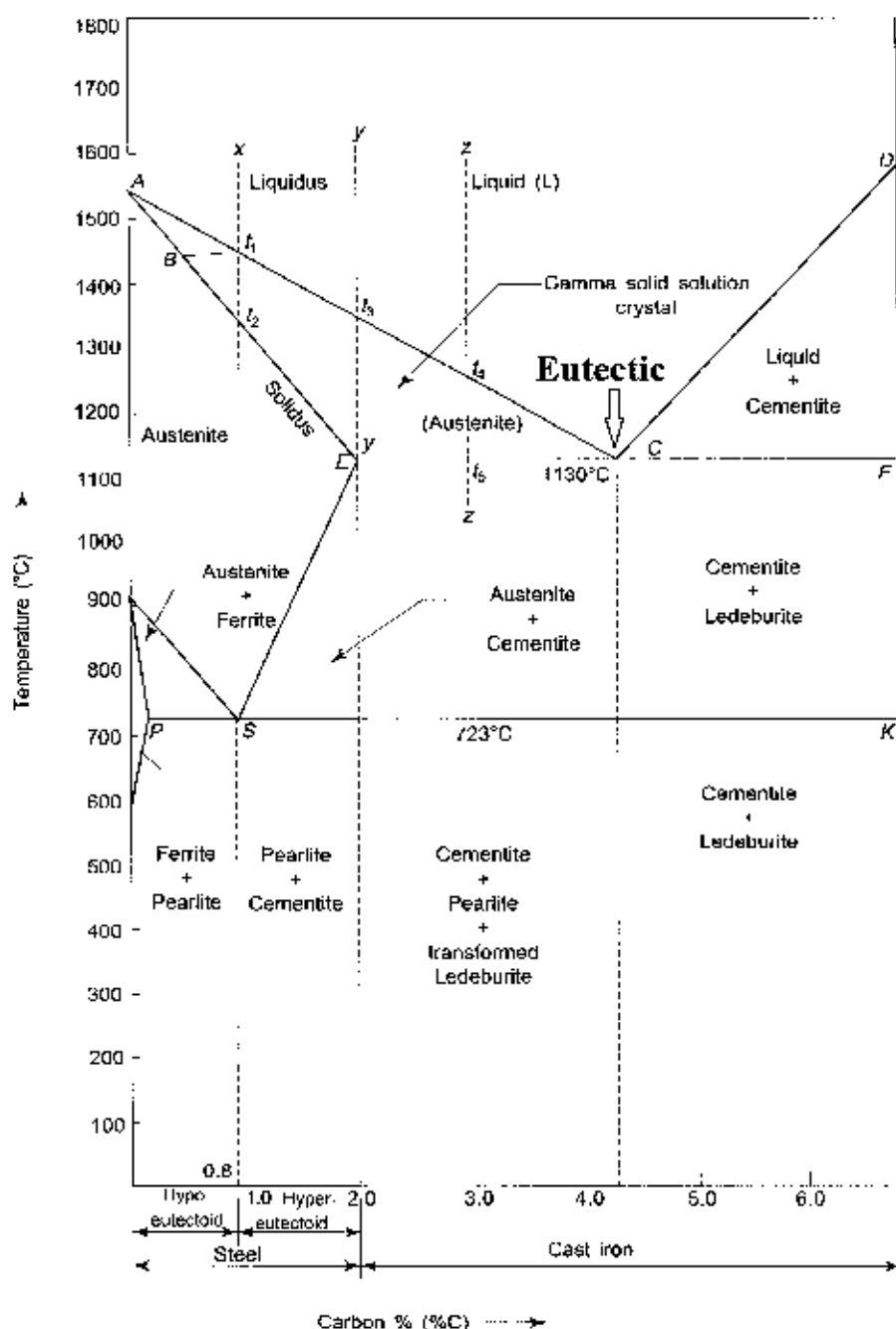


Figure 2.3 Modified iron-carbon equilibrium or phase diagram [17].

The microstructure of crystalline materials is defined by the type, structure, number, shape and topological arrangement of phases and/or lattice defects which are in most cases not part of the thermodynamic equilibrium structure.

Table 2.2 Constituents commonly found in cast iron microstructures, and their general effect on physical properties [18].

Constituent	Characteristics and effects
Graphite (hexagonal structure)	Free carbon; soft; improves machinability and damping properties; reduces shrinkage and may reduce strength severely, depending on shape.
Austenite (γ-iron)	Face-centered cubic crystal structure. The character of the primary phase, which solidifies from the oversaturated liquid alloy in dendrite form, is maintained until room temperature. Austenite is metastable or stable equilibrium phase (depending upon alloy composition). Usually transforms into other phases. Seen only in certain alloys. Soft and ductile, approximately 200 HB.
Ferrite (α-iron)	Body-centered cubic crystal structure. Iron with elements in solid solution, which is a stable equilibrium, low-temperature phase. Soft, 80–90 HB; contributes ductility but little strength.
Cementite (Fe_3C)	Complex orthorhombic crystal structure. Hard, intermetallic phase, 800–1400 HV depending upon substitution of elements for Fe; imparts wear resistance; reduces machinability.
Pearlite	A metastable lamellar aggregate of ferrite and cementite due to eutectoidal transformation of austenite above the bainite region. Contributes strength without brittleness; has good machinability, approximately 230 HB.
Ledeburite	Massive eutectic phase composed of cementite and austenite; austenite. Transforms to cementite and pearlite on cooling. Produces high hardness and wear resistance; virtually unmachinable.

2.4 Graphite

The properties of the gray cast iron are influenced greatly by the size, amount and distribution of the graphite flakes, which occur in the structure. These factors are controlled mainly by the composition, cooling rate and degree of nucleation of the iron. Slow cooling, higher carbon, silicon contents tend to produce more, and larger graphite flakes, a softer matrix structure, hence and lower strength [7]. The ASTM have developed a convenient standard for graphite (ASTM A247) [19], defining shape, size and distribution, and a similar standard has been issued by the International Standards Organization in ISO 945:1975 [20]. In ASTM 247 the flake graphite form has classified into five types, A through to E as shown in Figure 2.4.



Figure 2.4 Reference diagram for the distribution of graphite [21].

Type A graphite has uniform distribution and an apparent random orientation. It is the commonly preferred type of graphite giving optimum strength properties.

Type B graphite is in rosette groupings. The rosette pattern is typical of a moderate rate of cooling and is not uncommon in the more rapidly cooled surface areas of castings. The centers of rosettes generally contain fine graphite that formed because the start of solidification was temporarily undercooled. The latent heat of solidification raised the

temperature and solidification then continued in the normal manner with graphite flakes growing outward into the remaining liquid.

Type C graphite occurs in hypereutectic irons in which graphite forms in the liquid iron before eutectic solidification begins and is generally known as Kish graphite. It is characterized by coarse plates in heavy sections, and star shapes or clusters in light sections.







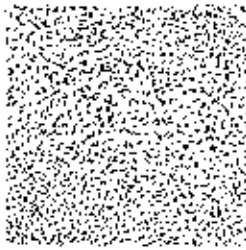
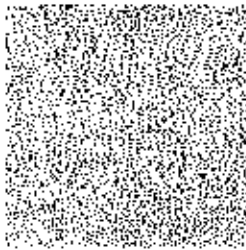
Type D graphite is often referred to as undercooled graphite and is normally associated with rapid rate of cooling and is particularly common in thin sections and surface regions. Both Type D and Type B are frequently associated with ferrite rather than pearlite, since the larger surface area of graphite available reduces the distance required for carbon diffusion during transformation from austenite in the critical temperature range.

Type E graphite occurs in strongly hypo-eutectic irons of low carbon equivalent with a dominant primary structure of austenite and a relatively lower amount of eutectic. The graphite formation is confined to the interstices between the austenitic dendrites so the graphite is described as interdendritic with preferred orientation.

Type A flaky graphite led to better erosion resistance than type D and, on the whole, spheroidal graphite led to better erosion resistance than flaky graphite. For those with the same graphite morphology and distribution, ferritic matrix results in less wear loss when eroded under large-angle impact; martensitic matrix results in less wear loss under oblique impact. Brittleness effect of both martensitic matrix and flaky graphite will cause maximum erosion rate to occur at higher impact angles [22].

Because of different graphite morphologies and distributions, graphite flake cast iron has higher damping capacity and heat conductivity but lower strength and toughness than spheroidal graphite cast iron [23]. These cast irons are often used in facilities that encounter particle erosion (e.g., automatic molding machine in casting industry, air pressure pump and gas delivery pipes). However, according to the authors' knowledge, literature reports on particle erosion of these cast irons are still limited. The limited reports mentioned above have all indicated that the erosion behavior of a cast iron is affected by its matrix structure. However, cast irons of different graphite morphologies and distributions may show diverse effects of matrix structure.

Figure 2.5 ASTM A-247 provides also a standard for evaluating the size of graphite. A chart shows standard graphite size from one to eight for one hundred [24].

<p>Size 1 Longest flakes 4 in. or more in length.</p> 	<p>Size 2 Longest flakes 2 to 4 in. in length.</p> 	<p>Size 3 Longest flakes 1 to 2 in. in length.</p> 	<p>Size 4 Longest flakes 1/2 to 1 in. in length.</p> 
<p>Size 5 Longest flakes 1/4 to 1/2 in. in length.</p> 	<p>Size 6 Longest flakes 1/8 to 1/4 in. in length.</p> 	<p>Size 7 Longest flakes 1/16 to 1/8 in. in length.</p> 	<p>Size 8 Longest flakes 1/16 in. or less in length.</p> 

Many methods to control the morphology, size and distribution of graphite flakes were used to improve the mechanical properties of the gray cast iron, such as modification, spheroiding, alloying and cooling rate, etc. [25–28].

Graphite is essentially an inert material and is cathodic to iron, consequently the iron will suffer rapid attack in even mildly corrosive atmospheres. The gray cast iron is subject to a form of corrosion known as graphitization, which involves the selective leaching of the iron matrix leaving only a graphite network. Even though no apparent dimensional change has taken place there can be sufficient loss of section and strength to lead to failure. In general gray cast iron is used in the same environment as carbon steel and low-alloy steels, although the corrosion resistance of gray cast iron is somewhat better than that of carbon steel. Corrosion rates in rural, industrial, and seacoast environments are generally acceptable. The advantage of gray cast iron over carbon steel in certain environments was the result of a porous graphite iron corrosion product film that forms on the surface. This film provides a particular advantage under velocity

conditions, such as in pipe lines. This is the reason for the widespread use of underground gray cast iron water pipes [29].

The gray cast iron is not resistant to corrosion in acid except for concentrated acids where a protective film is formed (Figure 2.6). It was not suitable for use with oleum (fuming sulfuric acid) because it has been known to rupture in this service with explosive violence.

The gray cast iron exhibits good resistance to alkaline solution such as sodium hydroxide and molten caustic soda. Likewise it exhibits good resistance to alkaline salt solutions such as cyanides, silicates, carbonates, and sulfides. Acid and oxidizing salts rapidly attack gray cast iron. The gray cast iron will contain sulfur at temperatures of 149-205°C (350-400°F). Molten sulfur must be air free and solid sulfur must be water free [30].

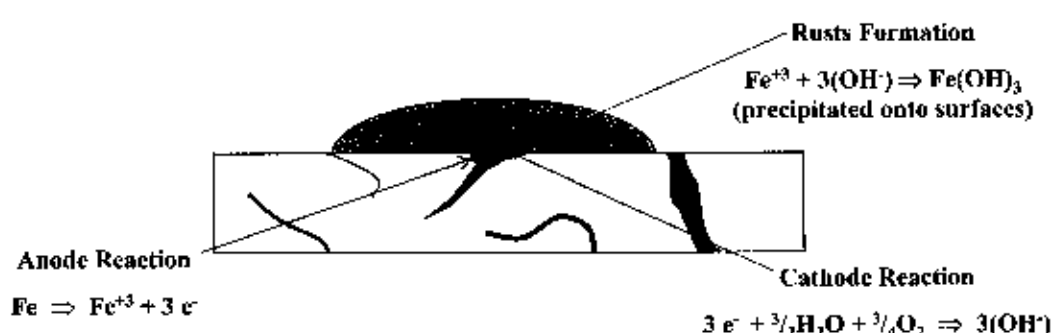


Figure 2.6 The difference in electrode potentials between the ferrite/iron carbide matrix and the graphite flakes is very large. This results in mini-galvanic cells with graphite as the cathode and the ferrite/iron carbide matrix as the sacrificial anode, which is the primary cause of the very poor corrosion resistance of gray cast iron [31].

The gray cast iron finds application in flue gas handling such as in wood, coal-fired furnaces, and heat exchangers. Large quantities are also used to produce piping which is buried. Normally gray cast iron pipe will outlast carbon steel pipe depending upon soil type, drainage, and other factors.

The microstructure of gray cast iron comprises free carbon in the form of graphite flakes and a ferritic or pearlitic matrix. The graphite flakes are formed during the solidification process and basically control the mechanical properties of the gray cast iron. The graphite flakes

confer low strength and toughness to the gray cast iron. There are several ways to change the mechanical properties of the gray cast iron.

2.5 Chemical composition

Chemical composition is another important parameter that influences the heat treatment of the gray cast irons. Silicon, for example, decreases carbon solubility, increases the diffusion rate of carbon in austenite, and usually accelerates the various reactions during heat treating. Silicon also raises the austenitizing temperature significantly and reduces the combined carbon content (cementite volume). Manganese, in contrast, lowers the austenitizing temperature and increases hardenability. It also increases carbon solubility, slows carbon diffusion in austenite, and increases the combined carbon content. In addition, manganese alloys and stabilizes pearlitic carbide and thus increases the pearlite content [32].

Sulfur in cast iron most commercial gray cast iron contain between 0.02 and 0.25 percent of weight. The effect of sulfur on the form of carbon is the reverse of silicon. The higher the sulfur content, the greater will be the amount of combined carbon, thus tending to produce a hard and brittle. Aside from producing combined carbon, sulfur tends to react with iron to form iron sulfide (FeS). This low-melting compound, present as thin inter dendritic layers, increases the possibility of cracking at elevated temperatures. High sulfur tends to reduce fluidity and often is responsible for the presence of blowholes (trapped air) in castings.

Manganese has a greater affinity for sulfur than iron, forming manganese sulfide (MnS). The manganese sulfide particles appear as small, widely dispersed inclusions which do not impair the properties of the casting. It is common commercial practice to use a manganese content of two to three times the sulfur content.

Manganese is a carbide stabilizer, tending to increase the amount of combined carbon, but it is much less potent than sulfur. If manganese is present in the correct amount to form manganese sulfide, its effect is to reduce the proportion of combined carbon by removing the effect of sulfur. Excess manganese has little effect on solidification and only weakly retard primary graphitization.

Phosphorus in gray cast irons contain between 0.02 and 0.15 percent of weight. Most of the phosphorus combines with the iron to form iron phosphide (Fe_3P). The condition

reduces toughness and makes the gray cast iron brittle, so that the phosphorus content must be carefully controlled to obtain optimum mechanical properties. Phosphorus increases fluidity and extends the range of eutectic freezing thus increasing primary graphite when the silicon content is high and phosphorus content is low. It is therefore useful in very thin castings where a less fluid iron may not take a perfect impression of the mold. If the silicon, sulfur, manganese, and phosphorus contents are controlled at proper levels, the only remaining variable affecting the strength of a pearlitic gray cast iron is the graphite flakes. Since graphite is extremely soft and weak, its size, shape, and distribution will determine the mechanical properties of the cast iron. It is the reduction of the size of the graphite flakes and the increase in their distribution that have accounted for the improvement in the quality of the gray cast iron [24].

2.6 The induction furnace

The induction furnace is a type of melting furnace that uses electric currents to melt metal. The induction furnace operates on a principle similar to a transformer where the furnace coil is the primary winding and the charge the secondary winding. There are several turns to the furnace coil whilst the charge is, in effect, a single short-circuited loop so that an alternating current applied to the coil will induce a much larger one in the charge. The resistance of the charge to the passage of the induced current produces a substantial heating effect. There is also a smaller heating effect due to magnetic permeability in magnetic material [33]. The electrical coil is placed around or inside of the crucible, which holds the metal to be melted. Often this crucible is divided into two different parts. The lower section holds the melt in its purest form, the metal as the manufacturers desire it, while the higher section is used to remove the slag, or the contaminants that rise to the surface of the melt.



Figure 2.7 Crucibles may also be equipped with strong lids to lessen how much air has access to the melting metal until it is poured out, making a purer melt.

2.7 Mechanical properties of gray cast iron

Mechanical properties of the gray cast iron are the body of knowledge which deals with the relation between internal forces, deformation and external loads. In the general method of analysis used in mechanical properties of the gray cast iron the first step is to assume that the structure was in equilibrium. The equation of static equilibrium were applied to the forces acting on some part of the body in order to obtain a relationship between the external forces acting on the structure and the internal forces resisting the action of the external loads.

The composition of the grey cast iron is subject to quantitative changes of its components, even so, the mechanical properties of the work pieces obtained should be stable [34] so that the subsequent machining process does not produce any problems. A usual practice in the cast iron manufacturing process was to leave the choice of chemical composition in the hands of the foundry man, who will choose the one which adapts best to the needs of the client, without forgetting, of course, that the requirements of his own foundry installations were determinant in order to obtain the desired properties [35]. It was largely done this way because in the cast iron manufacturing process, especially in the grey cast iron, the mechanical properties were not only affected by the chemical composition, but also by other factors such as: cooling speed, which can include the type of the mold used, the size of the flask, the time spent in the mold once the work piece has been poured, and the grade of sand removal once the work piece has been taken out of the mold [36].

The strength of the gray cast iron was determined by the strength of the steel-like matrix structure and the form and distribution of the graphite within it. The strength increases as the quantity of graphite decreases, as the carbon equivalent value decreases and as the eutectic cell number increases with inoculation. The strength also increases as the graphite flakes become finer and as the quantity of ferrite present in the matrix structure decreases, strength decreases as the cast section size increases and as the cooling rate decreases.

2.7.1 The Importance of cooling rate and section sensitivity

The structure and properties of the gray cast iron were significantly affected by cooling rate from the solidification temperature. There were two critical periods. First, the solidification range of 1250-1130 °C, during which graphite, austenite form and under certain circumstances white iron (cementite or chill). Second, the range between 720 and 650 °C when the matrix transforms into pearlite and/or ferrite.

The cooling rate of a casting is affected by several factors:

- (1) The initial pouring temperature.
- (2) The ratio of the surface area of the casting to its volume or mass.
- (3) The thermal conductivity and the heat capacities of the moulds and cores.

All of these factors were interrelated and affect properties and structure. Rapid cooling at the solidification temperature, for example in very thin section, or by the use of chills in the mould, promotes fine graphite and possibly white iron or chill. Continued rapid cooling through the critical temperature range of 720-650 °C, will promote a fine fully pearlitic matrix. However, the same iron, cast into a heavy section will solidify slowly, giving coarse graphite flakes. Very slow cooling through the critical range may result in full ferritic matrices. The latter situation sometime occurs when castings are stacked closely together after knockout, since partial annealing takes place as a result of very slow cooling.

The strength of the gray cast irons was mainly governed by the amounts and form of graphite flakes. Hence, strength depends on composition and the cooling rate of the latter being strongly affected by section thickness. The term used for this latter effect is section sensitivity. Section sensitivity was particularly important when designing castings. If the effects are not recognized the variations in tensile strength may result in inadequate properties in some sections or even failure.

2.7.2 Hardness and its relationship with tensile strength

The relationship between hardness and tensile strength for the gray cast iron as shows in Figure 2.7. There was a scatter of approximately $\pm 10\text{N/mm}^2$. The relationship needs to be established in each foundry and was only valid when the hardness determination was carried out at a constant position on a casting or test piece.

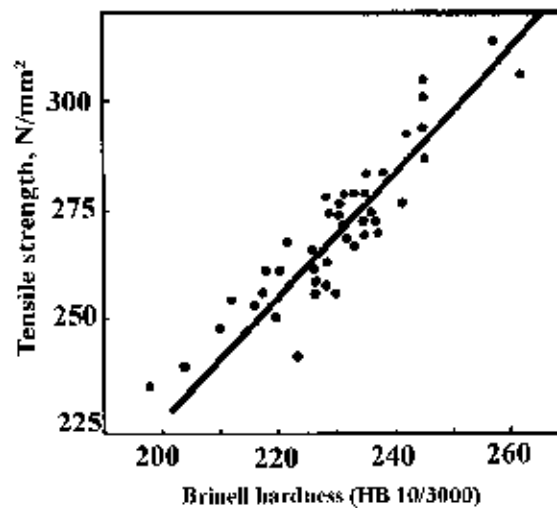


Figure 2.8 Approximate relationship between tensile strength and Brinell Hardness of irons produced in one foundry [7].

2.8 Heat transfer and solidification

The casting process was generally driven by the extraction of heat from the melt and the first section deals with heat flow during conventional casting, directional solidification, and rapid solidification processing. Next, the fundamentals of the freezing process were treated under the headings. When hot metal was poured into a mold, the rate at which it can lose heat is controlled by a number of thermal resistances. Figure 2.9 shows schematically the thermal conditions for a simple geometry of solidifying metal. In different parts of the sand mold system heat transfer may occur by conduction, convection or radiation. The formal treatment of this problem involves considerable complexity as a consequence of the continuous generation of latent heat at the moving solid-liquid interface and the variation of the physical properties of the metal-mold system with temperature.

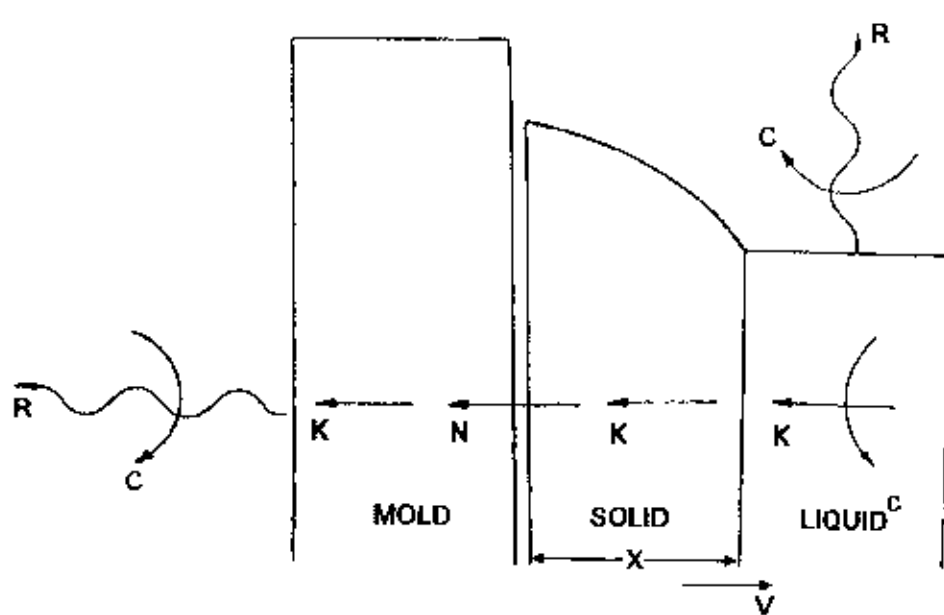


Figure 2.9 Thermal conditions for solidification of a simple geometry of a pure superheated liquid metal. In the figure, K corresponds to heat transfer by conduction, N to Newtonian heat transfer across the metal-mold interface, C to convective heat transfer, and R to heat transfer by radiation [16].

Nucleation during solidification can be defined as the formation of a small crystal from the melt that is capable of continued growth. From a thermodynamic point of view the establishment of a solid-liquid interface was not very easy. Although the solid phase has a lower free energy than the liquid phase, a small solid particle is not necessarily stable because of the free energy associated with the solid-liquid interface. The change in free energy corresponding to the liquid-solid transition must therefore include not only the change in free energy between the two phases but also the free energy of the solid-liquid interface.

The primary phase begins at the liquids temperature with the nucleation of austenite that grows in the form of dendrites, which develop and form the solidification units named primary grains or crystals [37-39]. Nucleation of the crystals takes place at the mold wall and in the inner melt originating the columnar and equiaxed grains respectively. Each grain is composed of one dendrite and has the same crystallographic orientation all over [39, 40].

After the passage of the solidification front, a variation of composition remains in the solid on a length scale characteristic of the dendritic growth that is called microsegregation.

This microsegregation pattern typically remains frozen in the solid due to the small ratio of the solute diffusion coefficients in the solid and liquid. The focus of this section is the prediction of the spacing associated with dendritic growth and the degree of microsegregation produced by that growth (Figure 2.10). These spacing are important in the selection of heat treatment times and temperatures for the homogenization of ingots as well as the properties of as cast materials. Thus the prediction of the microsegregation pattern is a fundamental goal of solidification modeling. Control of practical casting defects such as macrosegregation, porosity and hot tearing must start from control the cooling rate of casting process.

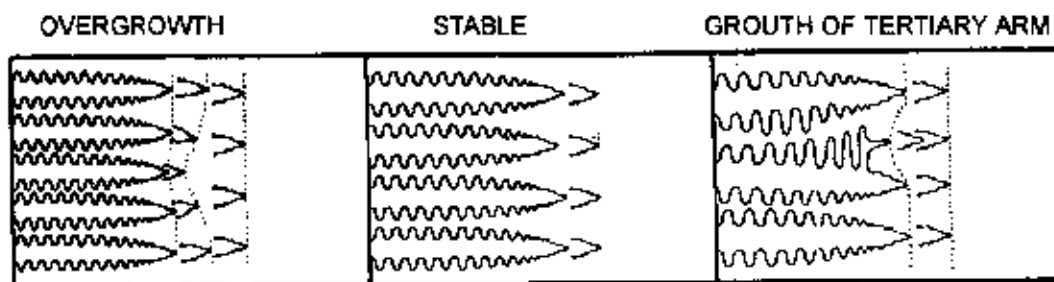


Figure 2.10 Schematic illustration of primary spacing adjustment mechanism for dendrites [16].

A dendrite in metallurgy is a characteristic tree-like structure of crystals growing as molten metal freezes, the shape produced by faster growth along energetically favorable crystallographic directions. This dendritic growth has large consequences in regards to material properties [41].

In the production process of the steel [42-47], the continuous casting process [48, 49] was an important one, which determines the quality of the steel. A reasonable cooling system of the continuous casting process will be helpful to improve the slab energy retention, to reduce the surface thermal stress and inner cracks, and to avoid the phenomenon of bulging. Many scholars have shown great interest in the analyses and optimizations for the cooling systems of continuous casting processes. Chen et al. [50, 51] built the coupled heat and stress models for solidification heat transfer processes, and optimized the cooling parameters for beam blank and billet continuous casting, respectively. The results showed that the cracks of the casting blanks after optimizations were reduced by 4.5% and 6%, and the water consumption in secondary cooling zone were reduced by 12.4% and 25%, respectively. Wang et al. [52]

developed a mathematical model for solidification heat transfer process based on actual distributions of the rollers and spray nozzles, and optimized the water consumption of the secondary cooling zone by using an advanced control strategy. The results showed that the water consumption preformed a trend of reduction, and the direct hot rolling temperature of the slab was increased.

CHAPTER 3

EXPERIMENTAL

In this thesis, I will describe the casting process using the induction furnace and pouring in molds. The mold was of cylindrical shape and made of sand with a mold wall thickness of 0.7, 1.5, and 2.8 inches. After that, the gray cast iron will be studied by X-ray diffraction (XRD), Scanning Electron Microscopy (SEM), Emission Spectrochemical analysis and mechanical testing.

3.1 The casting process

3.1.1 Composition of gray cast iron

The gray cast iron contained carbon, silicon, manganese, sulfur and phosphorus. Chemical compositions are normally to use for casting and the percent of weight is shown in Table 3.1. The raw material of melting is the iron scrap and mixed with inoculants before pouring iron melts into sand molds.

Table 3.1 Chemical composition (in wt%) of gray cast iron.

Composition	Carbon	Silicon	Manganese	Sulfur	Phosphorus
Percent of weight	2.50 - 4.00	1.00 - 3.00	0.60 - 0.80	0.02 - 0.25	0.02 - 0.15

Table 3.2 Chemical compounds of inoculants.

Composition	Silicon	Strontium	Zirconium	Calcium	Aluminium	Iron
Percent of weight	73 - 78	0.6 - 1.0	1.0 - 1.5	Max 0.1	Max 0.5	Balance

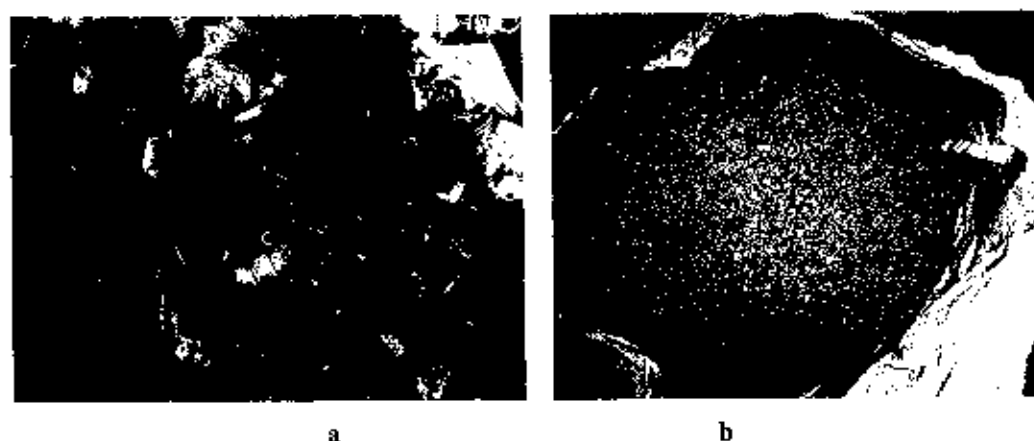


Figure 3.1 (a) The iron Scrap, and (b) Inoculants.

3.1.2 Induction furnace practice

The melting process by Induction Furnace, operates on a principle similar to a transformer where the furnace coil was the primary winding and the charge the secondary winding. There were several turns to the furnace coil (electromagnetic induction) whilst the charge was effected, a single short-circuited loop so that an alternating current applied to the coil will induce a much larger one in the charge. The resistance of the charge to the passage of the induced current produces a substantial heating effect. There were also a smaller heating effect due to magnetic permeability in magnetic materials. During induction, an electric current was passed through a metal coil which creates a magnetic field. When metal was introduced into the magnetic field, an electrical current passes through the metal and causes it to heat.

The coreless induction furnace has copper coils that were protected by a steel and magnetic shield, and kept cool by water circulating from a special cooling tower. A layer of refractory or difficult to melt material was placed above the coils and heated to the desired temperature. A crucible, which was a melting pot made of heat resistant material, was above the refractory. The metal to be melted was placed in the crucible and the heat produced by the electromagnetic charge melts the scrap.

After melting, the molten metal was poured into a mold. Some pouring methods were fully operated by human hands. Ours is mechanical with human intervention, while others are fully automated. Mechanical systems were more efficient for large scale projects, while manual pouring methods were more suited to low volume production lines.

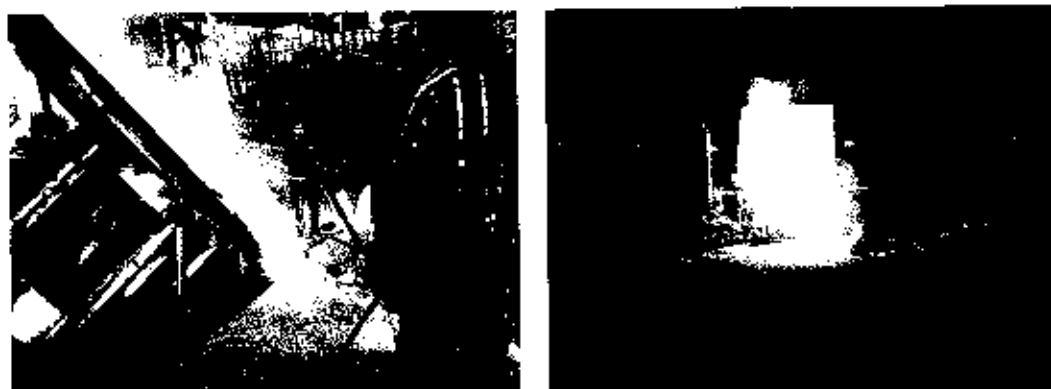


Figure 3.2 Starting the pouring process for the melted iron.

3.1.3 Mold preparation

In this process, the mold was made from river sand mixture with bentonite clay and water. The bentonite clay help to harden and hold the mold shape to withstand the pressures of the molten metal. The mold was of cylindrical shape and with a wall thickness of 0.7, 1.5, and 2.8 inches. Each size of mold wall thickness was prepared a set of sample, 5 samples of each mold size were made. When molten metal was poured into a mold, a pressure is exerted on the mold surface which depends on the dimensions of the mold. At a later stage, the gray cast iron expands on solidification, exerting a further pressure due to that expansion. After the sand casting was removed from the sand mold it was shaken out, all the sand was otherwise removed from the casting, and the gating system was cut off the part. The parts then undergo further processes such as machining and metal forming. An inspection was always carried out on the finished part to evaluate the effectiveness and satisfaction of its manufacture.

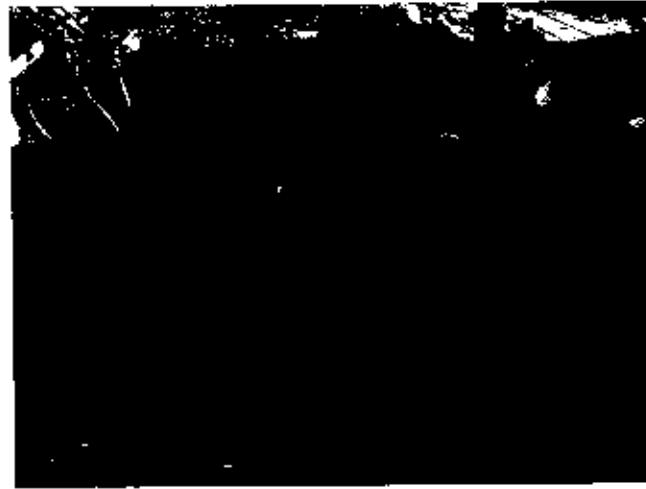


Figure 3.3 River sand mixture with bentonite clay and water.

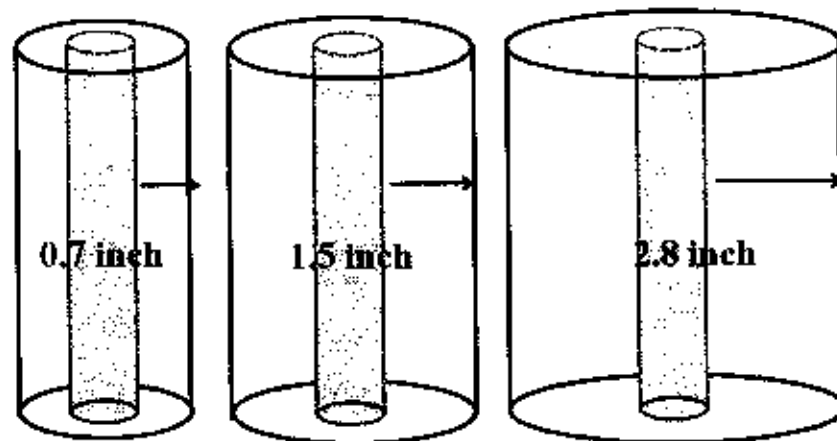


Figure 3.4 The wall thickness of 0.7, 1.5, and 2.8 inches.

Of specific interest to sand casting would be: the effect and dissipation of heat through the particular sand mold mixture during the casting solidification, the effect of the flow of liquid metal on the integrity of the mold and the escape of gases through the mixture. The sand usually has the ability to withstand extremely high temperature levels, and generally allows the escape of gases quite well. The moisture content was between 5 and 8 % used for making molds. This is because the sand mold has bonding power, but still absorbs almost as much water as active sand mold.

3.1.4 Thermocouple

The cooling rate of the solidified of gray cast iron was measured by using a digital multimeter equipped with K-type thermocouple. When the molten gray cast iron is poured into each mold it will start cooling. The thermocouples as the mold cools off are obtained from the thermocouple reading. A plot of temperature against time can then we analyzed to obtain the cooling rate for each mold thickness.

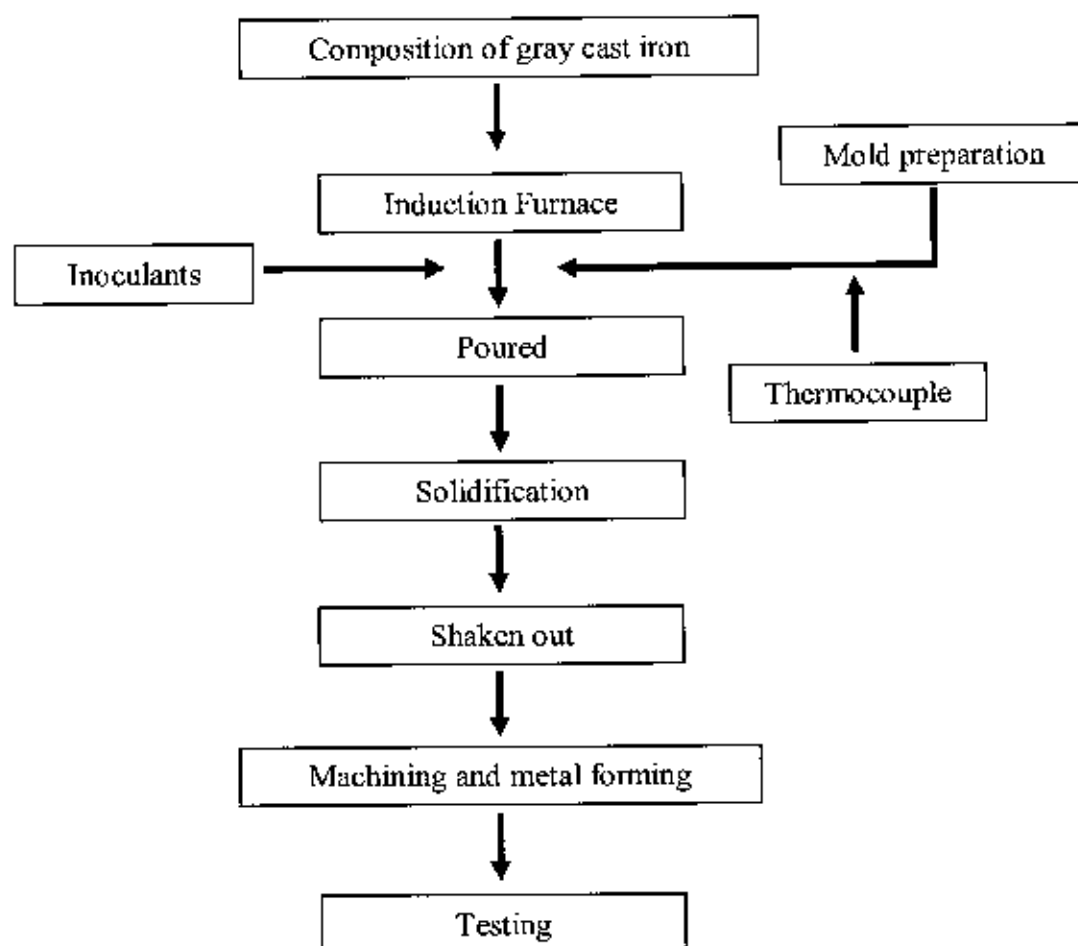


Figure 3.5 Diagram of casting process.

3.2 Process of mechanical preparation

3.2.1 Tensile strength

The tensile test of the specimens was carried out according to ASTM E8-04 standard as shown in Figure 3.6. The engineering stress on the bar is equal to the average uniaxial tensile force on the bar divided by the original cross-section area of bar.

$$\sigma = \frac{F}{A}$$

where σ is Engineering stress (MPa).

F is Average uniaxial tensile force (N).

A is Original cross-sectional (m^2).

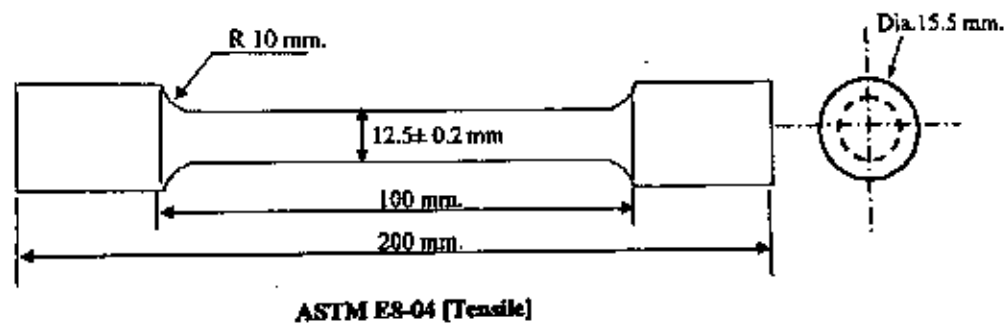


Figure 3.6 Dimensions of the tension test specimen.

3.2.2 Percentage elongation

Elongation is inversely proportional to tensile strength and hardness. The load necessary to cause this elongation was obtained from the elastic deflection of tensile testing, which measured by using hydraulic methods. The amount of elongation is expressed as a percentage of the elongation compare with the original gauge length. In reporting percent elongation, the original gauge length must be specified since the percent elongation will vary with gauge length. It is given by

$$\text{Percentage elongation} = \frac{L - L_0}{L_0} \times 100$$

where L is Final gauge length.

L_0 is Original gauge length.

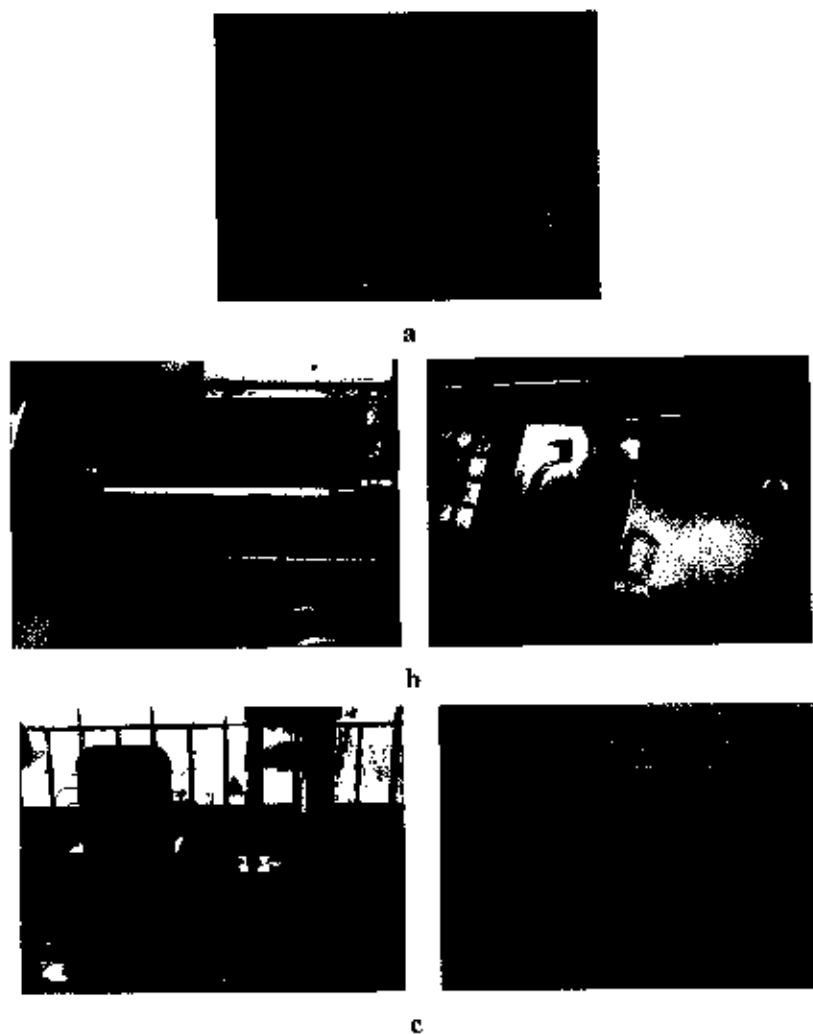


Figure 3.7 (a) The gray cast iron from the casting process, (b) It has been turning by a CNC machine, (c) Testing tensile strength and Percentage elongation.

3.3.3 The Rockwell test

The Rockwell test was used to determine the hardness by measuring the depth of penetration of an indenter under a large load compared to the penetration made by a preload. The Rockwell B scale use consists of a hand-operated vertical hydraulic press, designed to force a ball indenter into the test specimen. Standard procedure requires that the test be made with a ball of 10 mm diameter under a load of 150 kg.

$$\text{Rockwell B number} = \frac{130 \text{ depth of indentation}}{0.002}$$

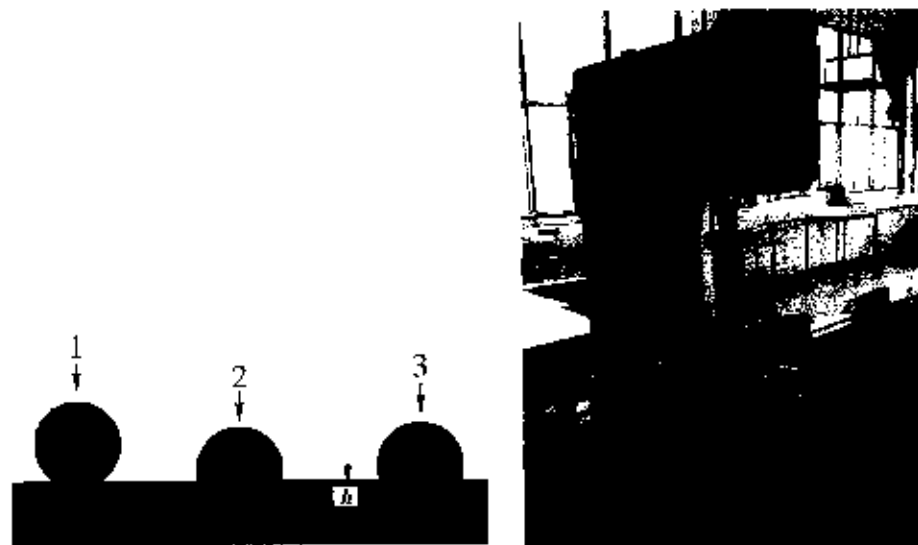


Figure 3.8 The steps in measurement of hardness with a sphere of steel and showed Rockwell scale hardness tester model: AR-10.

3.3.4 The heat transfer

Conduction heat transfer is the normal transfer of energy within solids. Conduction heat transfer also occurs through gases and liquids, but it then only predominates if the gases or liquids are stagnant or move slowly. The mathematical model for conduction heat transfer is Fourier's Law of conduction,

$$\dot{Q}_x = -\kappa A \frac{\partial T}{\partial x}$$

where Q_x is the heat transfer in the x direction of an area A due to the temperature gradient $\partial T/\partial x$. The thermal conductivity K is an index of ability of a material to conduct heat due to a temperature gradient in that material [53]. In SI unit, thermal conductivity is usually expressed in $W/m\cdot C$ and the heat transfer is W/m^2 . The thermal conductivity of the mixture of sand and clay was $0.81 W/m\cdot C$.

3.3 Emission Spectrometer

Emission Spectrochemical Analysis is a method of chemical analysis that uses the intensity of light emitted from a spark at a particular wavelength to determine the quantity of elements in a sample. The wavelength of the atomic spectral line gives the identity of the element while the intensity of the emitted light is proportional to the number of atoms of the element. The samples were prepared by chill casting process and the metal formed was shown in Figure 3.10 (a). Next, the samples test with ARL 3460 Fisons Instruments, shown in Figure 3.9. They were grounded with graphite to make them conductive. In traditional spark spectroscopy methods, a sample of the solid was commonly ground up and destroyed during analysis as shown in Figure 3. 10 (b). An electric arc or spark was passed through the sample, heating it to a high temperature to excite the atoms within it.



Figure 3.9 ARL 3460 Fisons Instruments.



Figure 3.10 (a) The samples before testing and (b) after testing.

3.4 Preparation of metallography and microstructures

3.4.1 Microstructure

In preparation, the samples were cut from the bulk the gray cast iron by CNC means of removing a part. Small parts may require only one cut and kept clear of the area of concern. In this case, the desired plane of observation is reached by careful cutting and polishing from heat effects. So, the coolant flow must be adequate to cool the sample. Fine grinding is usually performed with 240, 320, 400 and 600 grit abrasive papers. Fine polishing of the surface was carried out using a napped cloth which was moisturized with distilled water and charged with a very fine aluminum oxide powder (1 and 5 micron).

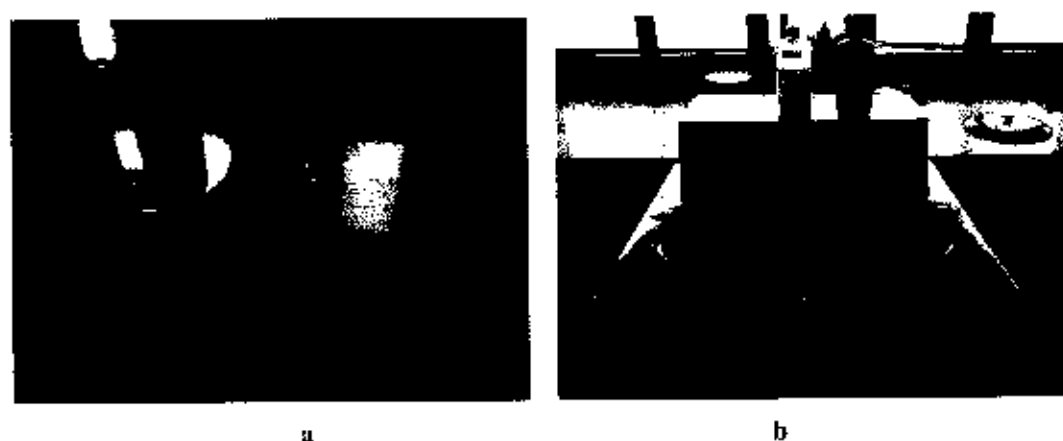


Figure 3.11 (a) The samples with polished surface and (b) Use of rotating wheel polisher.

Polishing could cause the microstructure to be less clearly defined, therefore more difficult to analyze. Etching is a technique used to restore the microstructure. The method requires a combination of solvent and chemical reagents. We prepared the etching process by using Nital (2% nitric acid in ethyl alcohol, HNO_3 1-5 ml, and Ethyl alcohol 100 ml) which helps selectively show various features of the microstructure and makes it visible through a microscope.



Figure 3.12 Etching by Nital in Chemical Fume Hood.

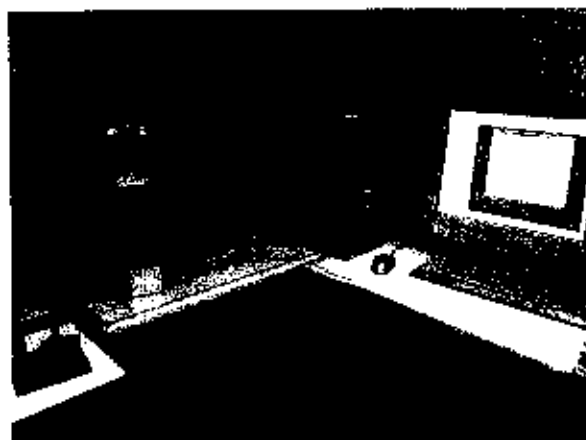


Figure 3.13 The microscopes connected with computer.

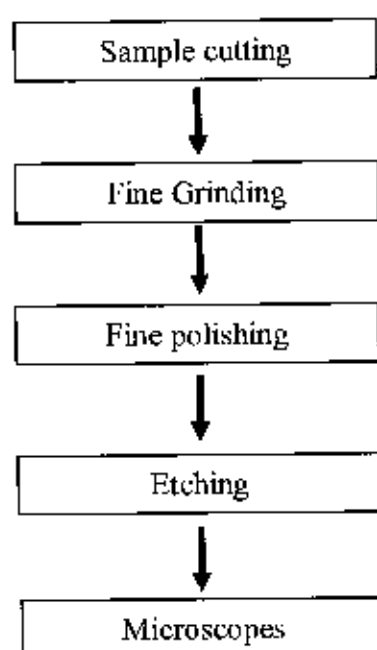


Figure 3.14 Diagram of Metallurgical specimen preparation

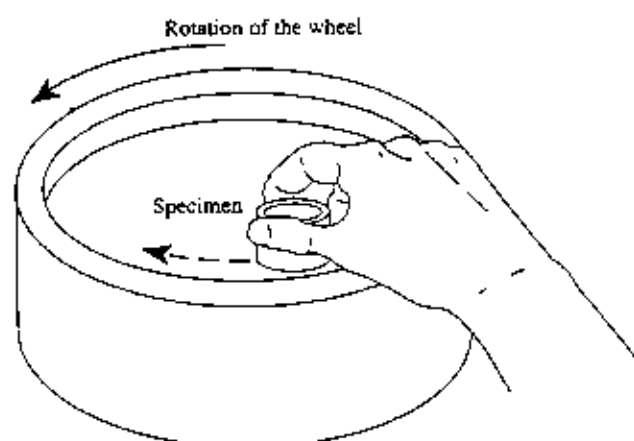


Figure 3.15 Direction of polishing on a rotating wheel.

3.4.2 Scanning Electron Microscopy (SEM) -

The microstructures of gray cast iron specimens were studied by using Scanning Electron Microscopy. SEM analysis was carried out by using JEOL JSM-5410 Scanning Electron Microscope equipped with EDS for quantitative elemental analysis.



Figure 3.16 A JEOL JSM-5410 Scanning Electron Microscopy.

3.4.3 X-ray Diffraction Analysis (XRD)

X-ray diffraction (XRD) technique was used to examine crystalline phase identification. The position of a diffraction line (peak position) and the shape and width of a diffraction line, the so-called diffraction-line broadening (peak width), can be used to determine many important microstructure parameters, such as the concentration of the gray cast iron element dissolved in the matrix phase, the crystallite size (of the precipitating phase) and the concentration of defects as vacancies and dislocations. X-ray data were collected by using PHILIPS X'Pert MPD X-ray diffractometer at 40 kV and 30 mA and using Cu K_{α} radiation with the wavelength of 1.54 Å.



Figure 3.17 PHILIPS X'Pert MPD diffractometer.

CHAPTER 4

RESULTS AND DISCUSSION

The results of cooling rate and mechanical property will be present in this chapter. The emission spectrochemical technique, microstructures, scanning electron microscopy (SEM), and x-ray diffraction (XRD) will be analyzed and discussion.

4.1 Mechanical property

Tensile tests were performed on the gray cast iron specimens. Table 4.1 shows the average tensile test results of three specimens made of 0.7, 1.5, and 2.8 inch mold wall thickness. As shown in Table 4.1, the results revealed that the tensile properties of the gray cast iron improved due to low cooling rates. The maximum of tensile strength, hardness and percentage elongation were 255.06 MPa, 210 Brinell and 0.82% of specimens with 1.5 inches mold wall thickness. The heat transfer of specimens casted with 0.7 inches mold wall thickness is 501.66 watts greater than that of 1.5 and 2.8 inch mold wall thickness.

Table 4.1 The average of the mechanical testing.

Size	Tensile strength (MPa)	Elongation at break (%)	HB (Brinell)	\dot{Q} , (W)
0.7 inches	243.92	0.71	210	501.66
1.5 inches	255.06	0.82	210	476.57
2.8 inches	253.31	0.80	205	453.65

The plots of the cooling rate curves as a function of time were shown in Figure 4.1. Constant temperature ranges were 668 °C, 680 °C, and 719 °C for 1.5, 0.7 and 2.8 inch mold wall thickness, respectively.

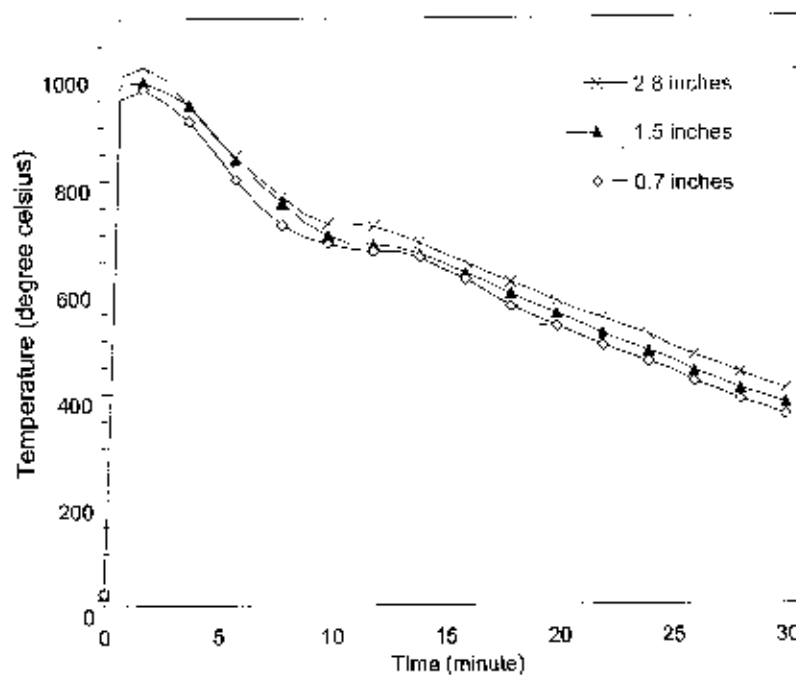


Figure 4.1 The plots of the cooling rate curves of the different mold wall thickness obtained.

4.2 Emission spectrochemical technique

The sample was clamped in place and sparked to generate a spectrum, which leaves burn marks on the samples and sparked three times on the surface. The results of the analysis of the gray cast iron were shown in Table 4.2. Higher carbon irons were less likely to shrink and have better fluidity than lower carbon irons. On the other hand, attempting to correct shrink with higher carbons can lead to other problems, especially in big castings. High carbons and slow cooling rates can lead to a condition called carbon flotation. Graphite typically forms first during solidification and was lighter than iron. If the solidification of the entire casting was slow enough, the graphite floats toward the surface of the casting. Silicon was like carbon in many respects. While silicon control in a cupola can be difficult, in induction melting it was relatively easy. Also like carbon, the higher the silicon the more likely larger graphite will occur as well as more ferrite in the matrix. When silicon becomes very high it hardens the ferrite and can increase the hardness of the iron. With silicon contents over 3% that temperature can be raised so high that castings will be brittle at room temperature.

Table 4.2 Chemical compositions of the gray cast iron.

Elements	Weight percent (Wt%)			
	Position 1	Position 2	Position 3	Average
C	3.185	3.112	3.126	3.141
Si	2.652	2.638	2.681	2.657
Mn	0.364	0.367	0.367	0.366
P	0.077	0.079	0.079	0.079
S	0.053	0.060	0.058	0.057
Cr	0.126	0.128	0.128	0.127
Mo	0.017	0.017	0.017	0.017
Ni	0.079	0.077	0.080	0.078
Al	0.008	0.008	0.008	0.008
As	0.002	0.002	0.002	0.002
Fe	93.149	93.220	93.157	93.175

$$\begin{aligned}
 \text{Carbon equivalent (CE)} &= \text{C}\% + \frac{(\text{Si}\% + \text{P}\%)}{3} \\
 &= 3.141 + \frac{(2.657 + 0.079)}{3} \\
 &= 4.053
 \end{aligned}$$

The carbon equivalent was 4.053 which mean that the gray cast iron was hypo-eutectic. The solidification of hypo-eutectic of the gray cast iron starts with the nucleation of primary austenitic crystals. A solid solution of carbon in austenite which crystallites in the form of dendrite.

4.3 Metallography and Microstructures

The graphite flakes of the specimens were observed using an optical microscope after polishing and etching as shown in Figures 4.2 - 4.4 for type a graphite. The large graphite flakes seriously interrupt the continuity of the pearlitic matrix, thus reducing the strength and ductility of the gray iron. The small graphite flakes were less damaging and therefore generally preferred. Flake graphite was subdivided into five types (patterns), which were designated by the letters A through E. The orientation distribution of Type A graphite is random. It was the commonly preferred type of graphite giving optimum strength properties.

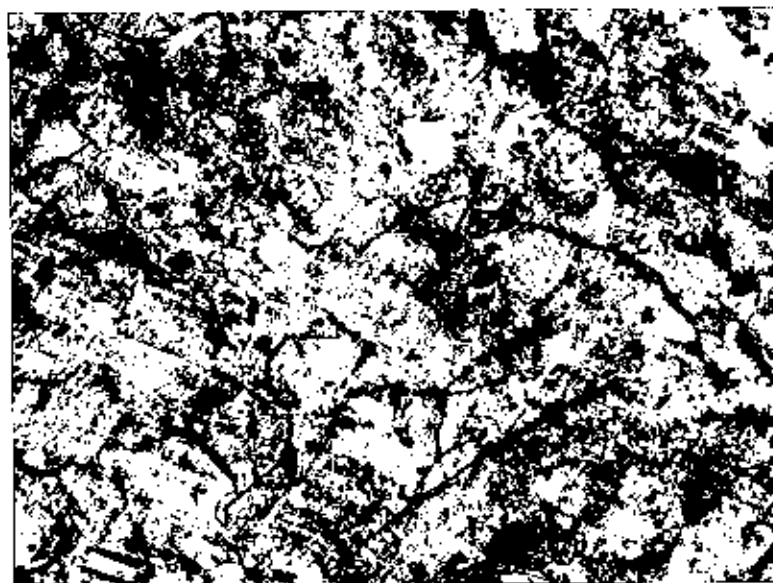


Figure 4.2 Microstructure of solidified gray cast iron from the mold wall thickness 0.7 inch.

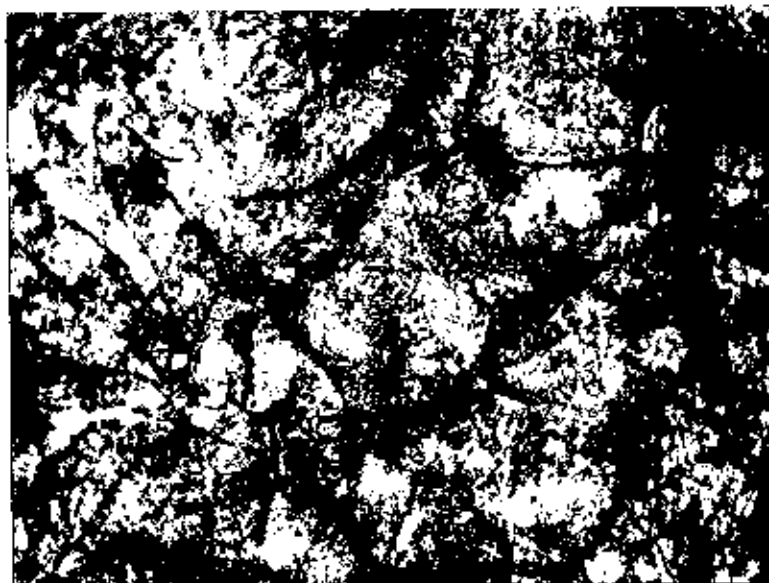


Figure 4.3 Microstructure of solidified gray cast iron from the mold wall thickness 1.5 inch.

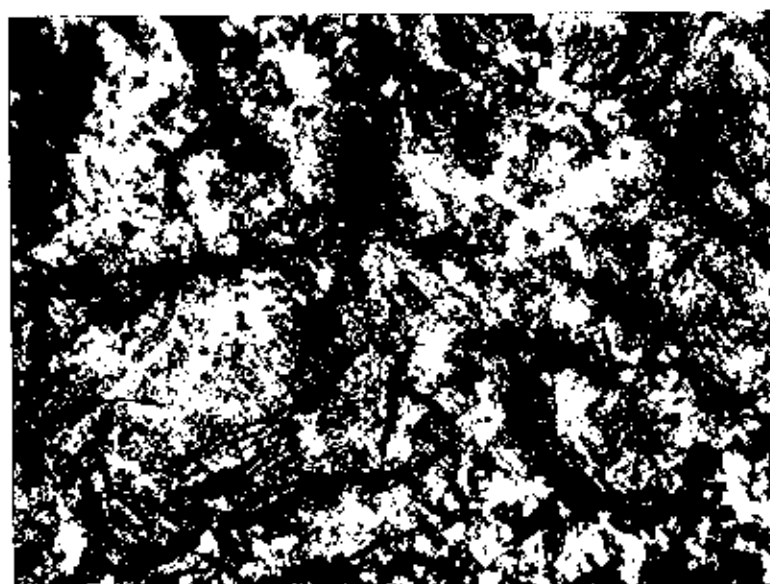


Figure 4.4 Microstructure of solidified gray cast iron from the mold wall thickness 2.8 inch.

Ferrite is a relatively soft constituent and is therefore undesirable when high strength and good wear resistance is required. A substantial amount of ferrite can be associated with fine forms of graphite, such as undercooled and rosette forms. In a mixed matrix structure, ferrite will often occur adjacent to graphite because the carbon that was in solution in the ferritic areas can diffuse to precipitate on the existing graphite flakes during cooling. Pearlite consists of alternate lamellae of soft ferrite and cementite. The hardness of pearlite varies within the range of approximately 170-300 HB. It is a desirable constituent when high strength and good wear resistance are required. Hardness increase with increasing fineness of the laminations.

4.4 Scanning electron microscopy analysis

Figures 4.5, 4.6 and 4.7 show the tensile fracture surfaces of the gray cast iron specimens. Figure 4.5 (b) shows the fracture surface of the gray cast iron similar to flowers. The dendrite in metallurgy is a characteristic tree-like structure of crystals growing as molten metal freezes, as shown in Figure 4.5 (a) produced by fast growth along energetically favorable crystallographic directions. The dendrite has been established that crystals grow with the highest rate along the planes and directions where atoms are packed more closely. Thus, long branches grow first, which are called the first-order dendrite axes. Then second-order axes branch off from them and third-order axes from the second-order ones, and so on. Finally, the metal remaining between dendrite axes solidifies. If there is enough liquid metal to fill in inter axial spaces or opened end of a mould where a shrinkage cavity forms, some crystals may retain the dendrite shape. This dendrite growth has large consequences in regards to material properties.

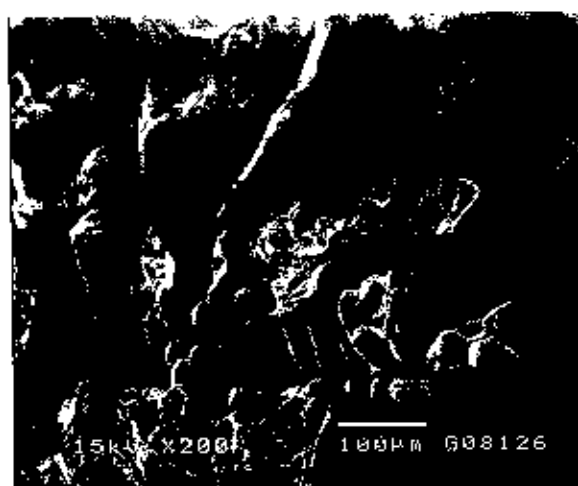
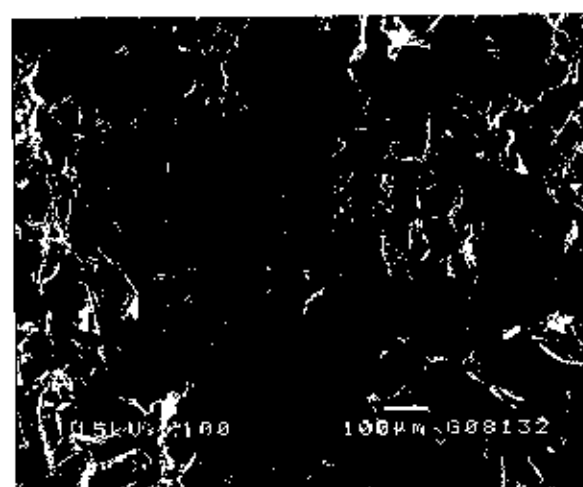
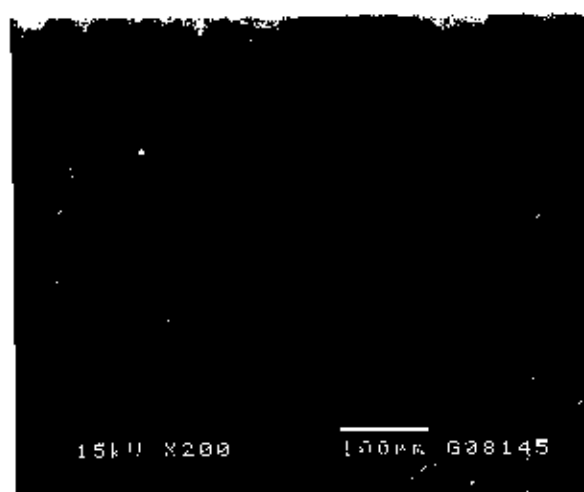
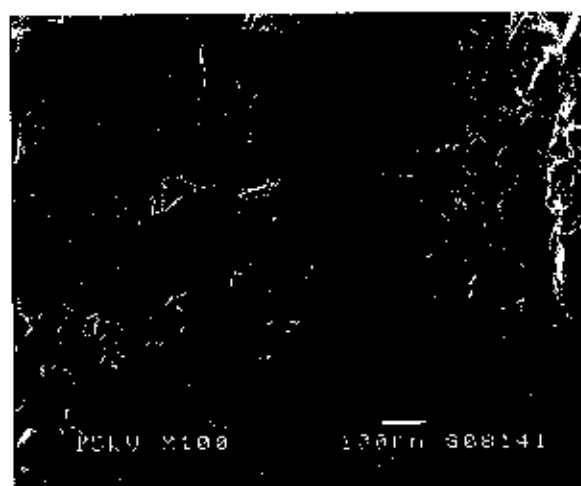
**a****b**

Figure 4.5 Tensile fracture surfaces of the mold wall thickness of 0.7 inches.



a



b

Figure 4.6 Tensile fracture surfaces of the mold wall thickness of 1.5 inches.

The main part of the fracture surface is the boundary between the graphite and metal matrix. Figure 4.5 and 4.6 show the fracture surface of graphite. The total elongation of the gray cast iron is about 0.71-0.80 %. The low value of total elongation yields a result in low tensile strength that causes low ductility and is brittle.

4.5 X-ray diffraction patterns

The XRD patterns of the specimens were shown in Figure 4.8. The XRD patterns show a single phase of cubic $Im\bar{3}m$ (ferrite) space groups. The data analysis reveals that the lattice parameter of the specimens was 2.86 \AA . The optical emission spectroscopy test shows that the specimens are composed of Fe 93.17%, C 3.14 %, and Si 2.65 %. $Im\bar{3}m$ (ferrite) space groups are a soft and ductile phase. Basically, this was a BCC iron phase with very limited solubility of carbon.

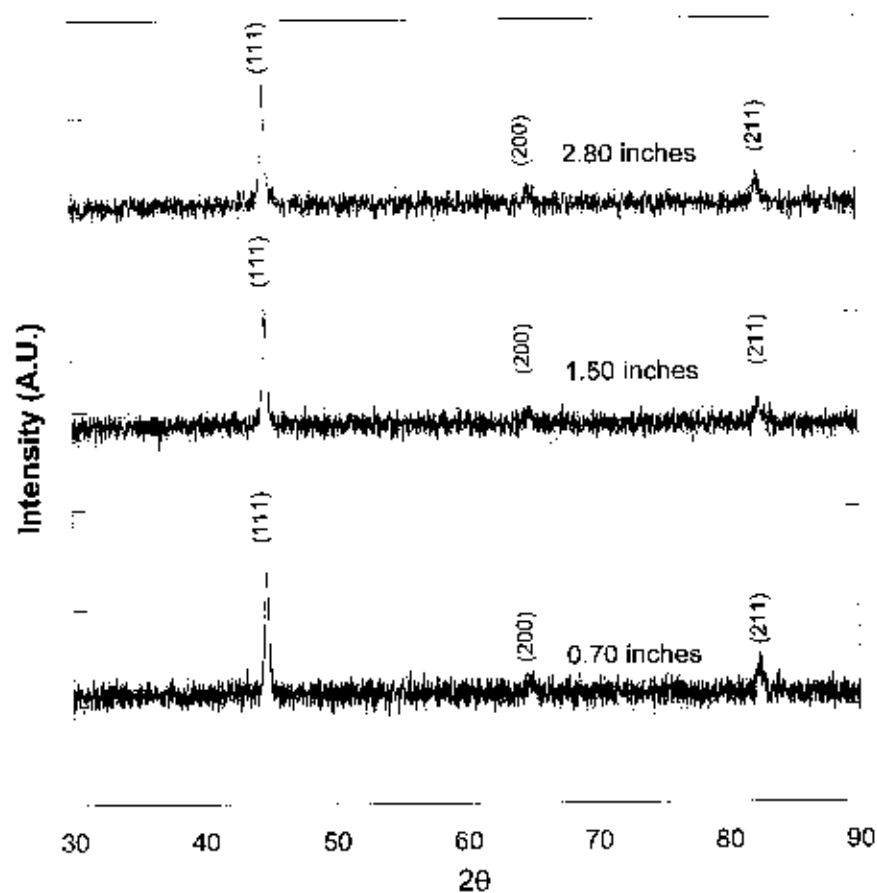


Figure 4.8 XRD pattern of the gray cast iron specimen.

CHAPTER 5

CONCLUSIONS AND SUGGESTION

We have succeeded in controlling the cooling rate to increase the tensile strength of gray cast iron. The evaluation of the gray cast iron with different cooling conditions shows that the cooling rate has an effect on the tensile strength, microstructure and hardness Brinell (HB). We prepared the mold wall thickness of 0.7, 1.5, and 2.8 inches to determine the cooling rate. The results of this work indicate that the tensile strength, hardness and percentage elongation of the gray cast iron is optimized when the mold wall thickness of 1.5 inches was used. The lowest of the tensile strength and the percentage elongation were 243.92 Mpa and 0.71% of specimens, respectively with 0.7 inch mold wall thickness. However, the heat transfer of the specimens casted with 0.7 inch mold wall thickness is 501.66 watts greater than that of 1.5 and 2.8 inch mold wall thickness. Thus, the structure of the gray cast iron was cast with 0.7 inch mold wall thickness has characteristic dendrite structure. The large dendrite growth causes the decreases of tensile strength and percentage elongation.

The structures of all specimens are single phase of iron with cubic $Im - 3m$ space group. It was body - centered cubic (BCC) crystal structure or ferrite. This crystalline structure the gray cast iron has magnetic properties and was the classic example of a ferromagnetic material.

The graphite flakes of all specimens were present in type A. The large graphite flakes seriously interrupt the continuity of the pearlitic matrix that result in reducing the strength and ductility of the gray cast iron. The small graphite flakes are less damaging and therefore generally preferred. The orientation distribution of Type A graphite was random. It was the commonly preferred type of graphite giving the optimum strength properties.

SEM images with 0.7 inch mold wall thickness show that the solidification of flake and graphite were dominated by the growth of the dendrite forming the grain pattern similar to that of most gray cast iron. This gives additional support to the solidification mechanisms proposed earlier.

Suggestion for the casting process is the mold wall thickness between 1.5 and 2.8 inches casting processes (The mold made from sand mixing with betonics) can be used in foundary manufactures. These sizes of the mold thickness help to control the cooling rate to get good tensile strength and hardness. The addition of inoculants in liquid cast iron grey cast irons helps to improve the homogeneity of the cast iron structure, enhance mechanical properties and decrease the failure of gray cast iron products.

REFERENCES

REFERENCES (CONTINUED)

- [16] Robert W. CAHN and Peter HAASEN. PHYSICAL METALLURGY, Fourth edition. United States of America: Elsevier Science, 1996.
- [17] S. L. Kakani and Amit Kakani. Material Science. New Delhi: New Age International Publishers, 2004.
- [18] O. J.A. Nelson. Cast Irons, Metallography and Microstructures. USA: ASM Handbook, 1985,
- [19] ASTM. Standard Test Method for Evaluating the Microstructure of Graphite in Iron Castings. USA: ASM Handbook, 1998.
- [20] ISO. Cast iron - Designation of microstructure of graphite, Switzerland: ISO, 1975.
- [21] Japan Industrial Standards. Standard for Ductile Iron. Japan: JIS, 1995.
- [22] W.S. Dai, L.H. Chen and T.S. Lui. "A study on SiO particle erosion of flake graphite and spheroidal 2 graphite cast irons", Wear. 239: 143–152, 2000.
- [23] H.T. Angus. Cast Iron: Physical and Engineering Properties. London: Butterworths, 1976.
- [24] Aver, Sidney H. "Introduction to Physical Metallurgy" 2nd Ed. New York: McGraw-Hill, 1987.
- [25] F.W. Charles and J.O. Timothy. Iron Castings Handbook. USA: Iron Casting Society Inc., 1981.
- [26] A.R. Ghaderi, M. Nili Ahmadabadi and H.M. Ghasemi. "Effect of graphite morphologies on the tribological behavior of austempered cast iron", Wear. 255: 410–416, 2003.
- [27] K. Edalati, F. Akhlaghi and M. Nili-Ahmadabadi. "Influence of SiC and FeSi addition on the characteristics of gray cast iron melts poured at different temperatures", Mater. Process. Technol. 160: 183– 187, 2005.
- [28] M. Ramadan and M. Takita, H. Nomura. "Effect of semi-solid processing on solidification microstructure and mechanical properties of gray cast iron", Mater. Sci. Eng. 417: 166–173, 2006.
- [29] Philip A. Schweitzer, P.E. Metallic materials physical, Mechanical, and corrosion properties. New York: MARCEL DEKKER Inc., 2003.

REFERENCES (CONTINUED)

- [30] P.A. Schweitzer. Corrosion Resistance Tables, 4th ed. Vols. 1-3. New York: Marcel Dekker, 1995.
- [31] Mark Ihm. Introduction to Gray Cast Iron Brake Rotor Metallurgy. USA: TRW Automotive, 2003.
- [32] K.V. Sudhakar. "Cast iron component failure: A metallurgical investigation", Archives of Foundry Engineering. 12: 67-70, 2012.
- [33] M. W. Hubbard, A.I.M. Steelmaking for Steel Founders: Induction Furnace Practice. USA: Steel Castings Research and Trade Association, 1972.
- [34] American Society for Metals. Metals Handbook: Melting and Casting of Ferrous Metals. USA: ASM 8th ed., 1970.
- [35] S. Kantz. Trends in melting plant practice in the USA, in: BCIRA International Conference on Progress in melting cast irons. USA: Warmick, 1990.
- [36] I. Minkotf. The Physical Metallurgy of Cast Iron. London: John Wiley & Sons, 1983.
- [37] L. Elmquist. "Factors Influencing the formation of Shrinkage Porosity in Grey Cast Iron", Licentiate Thesis. Göteborg, Sweden: Chalmers University of Technology. 1: 24-26, 2008.
- [38] R.H. Heine and C.R. Looper. "On Dendrites and Eutectic Cells in Grey Iron", Modern Casting, 4(56): 185-191, 1969.
- [39] G.L. Rivera, R.E. Boeri and J.A. Sikora. Solidification of Gray Cast Iron. Argentina: National University of Mar de Plata, 2003.
- [40] T.S. Piwonka. Casting, Metals Handbook, 2nd Ed. USA: ASM International, 1998
- [41] J. A. Dantzig and M. Rappaz. Solidification. USA: EPFL Press, 2009.
- [42] Marcio MC, Roberto S and Ernst W. "Exergy accounting of energy and materials flows in steel production systems", Energy. 26(4): 363-384, 2001.
- [43] Yin R. "The essence, functions, and future development mode of steel manufacturing process", Sci China Ser E-Tech Sci. 38(9): 1365-1377, 2008.
- [44] Yin, R. Metallurgical process engineering. New York: Springer, 2011.

REFERENCES (CONTINUED)

- [45] Gao C, Wang D and Du T. "Optimization and evaluation of steel industry's wateruser system", J Clean Prod. 19(1): 64-9, 2011.
- [46] Zhang F. "Study and design on clean steel and production platform", Appl Mech Mater. 161(37): 37-41, 2012.
- [47] Strczov V, Evans A and Evans T. "Defining sustainability indicators of iron and steel production", J Clean Prod. 51: 66-70, 2013.
- [48] Mishra P, Ajmani Sk, Kumar A and Shrivastava KK. "Review article on physical and numerical modeling of sen and mould for continuous slab casting", Int J Engng Sci Tech. 4(5): 2234-2243, 2012.
- [49] Lee Peter D, Ramirez-Lopez PE and Mills KC. "Review: the "Butterfly effect" in continuous casting", Ironmak Steelmak. 39(4): 244-253, 2012.
- [50] Chen W, Zhang Y and Zhang C. "Thermo-mechanical simulation and parameters optimization for beam blank continuous casting", Mater Sci Eng. 499(1-2): 58-63, 2009.
- [51] Chen W, Zhang Y and Wang B. "Optimization of continuous casting process parameters based on coupled heat and stress model", Ironmak Steelmak. 37(2): 147-54, 2010.
- [52] Wang Z, Yao M, Zhang X and Wang X. "Optimization control for solidification process of secondary cooling in continuous casting steel", Appl Mech Mater. 263: 822-827, 2012.
- [53] Rolle, Kurt C. Heat and Mass Transfer. New Jersey: Prentice-Hall, 2000.

APPENDIX



The 4th UBRU International Research Conference
on "An Integration of ASEAN Local Wisdom to International"

13 March 2014

Ubon Ratchathani Rajabhat University, THAILAND
Organized by Ubon Ratchathani Rajabhat University 2014

Venue : Ubon Ratchathani Rajabhat University, Ubon Ratchathani, Thailand

Website : www.ubruirc2014.com E-mail : ubruirc2014@gmail.com

Tel. 045 352000 ext. 1120

The Structures and Properties of Cooling-Rate Controlled Gray Cast Irons by Different Mold Wall Thickness.

Kittikhun Seawsakul^{1a}, Wichan Piwbang¹, and Udom Tipparach^{2b}

¹ Student, Master of Science Program in Physics, Faculty of Science, Ubonratchathani University, Ubonratchathani, Thailand

² Assist. Prof. Department of Physics-Science, Faculty of Science, Ubonratchathani University, 85 Satholmark Rd. Warinchamrap UbonRatchathani, Thailand 34190 Tel. 045-353401-4, Fax 045-353422

^a inthezone555@hotmail.com, ^b udomt@hotmail.com

Abstract

We have investigated the structures and properties of cooling-rate controlled gray cast irons by different mold wall thickness. The cast iron specimens were made by controlling the cooling rate in the solidification process. The mold was cylindrical in shape and made of sand. The process of the heat transfer of the materials was investigated. The heat transfer rate was considered as the radial thickness of the mold wall. The X-ray diffraction (XRD) technique was used to identify the phase and optical microscope used to study the microstructure. Optical emission spectroscopy was employed to examine the constituent of the specimens. Three gray cast irons with the mold wall thickness of 0.7, 1.5, and 2.8 inches were casted and tested for tensile strength. The results showed that the specimens made of 1.5 inch radial mold thickness yielded the highest tensile strength.

Keywords: Cooling-rate, Tensile Strength, Gray Cast Iron, X-ray diffraction

1. Introduction

Gray cast iron has become a popular cast metal material which is widely applied in modern industrial manufacture because its good castability, wear resistance, low melting point, machinability, high damping capacity, and low cost. The microstructure of gray cast iron is characterized by graphite flakes dispersed into the matrix. Industrial casting practice can influence nucleation and growth of graphite flakes, so that types and sizes increase the desired properties. The amount of graphite and distribution of graphite lamellas are essential in determining the mechanical quality of gray cast iron (L. Collini, et al., 2008; J.R. Davis et al., 1985). Thus, it is important to control the flake graphite morphology that has direct influence on the properties of gray cast iron. The structure of gray cast iron depends on chemical composition, inoculants and physical properties. Some researchers have studied the unidirectional solidification process to improve the mechanical properties of gray cast iron. For example, B.A Ceccarelli et al. (2004) and J.V. Giacchi et al. (2007) have modified the morphology of graphite flakes by inoculating the iron melt to improve the fracture toughness or impact toughness and applying austempering heat treatments to improve the fracture toughness of monolithic gray cast iron.

High cooling rates in producing fine structures resulted in increasing of high-strength cast alloys. The undercooling of a melt to a lower temperature increased the number of effective nuclei relative to the growth rates and the final being restricted by the rates at which the latent heat of crystallization can be dissipated. The refining influence of an enhanced cooling rates applied to grain sizes and to substructures.

This work presented the effect of the design of the cooling rate control on the tensile strength, morphology, and microstructure of the specimens extracted from industrial castings made of gray cast iron, and produced by different wall thickness of the

sand molds. The cooling rate was used to control the flake graphite morphology. Then, the mechanical properties of the gray cast iron were tested.

2. Research Methodology

2.1 Materials and casting procedures

The specimens of gray cast iron were casted with 0.7, 1.5, and 2.8 inch wall thickness to obtain different cooling rates. The specimens with the composition (mass percent) of: C 3.141%, Si 2.657%, Mn 0.366%, P 0.079%, S 0.057%, and others. The casting was made at 1350-1400 °C. The molds were designed in cylindrical shape and made by river sand. K-type thermocouples were mounted in the middle of cylindrical shape to measure real cooling rate temperatures. After the melted cast iron was poured into the molds, the cast iron samples were cooled to room temperature naturally. The temperatures of the cooling rates were collected as a function of time. The specimens of metallographic examination using an optical microscope were prepared to examine the flake morphology and matrix microstructure of the composites. The surfaces of the metallographic specimens are prepared by methods of polishing and etching. After the preparation, the distribution of graphite flakes was examined under an optical microscope at a magnification of 100×. XRD method using X'Pert plus with wavelength of 1.54 Å was used to study phase and microstructure of the specimens. Optical Emission Spectroscopy was used to probe the constituent of the specimens.

2.2 Mechanical properties

1. Tension tests of the specimens were carried out according to ASTM E8-04 standard as shown in Fig.1.

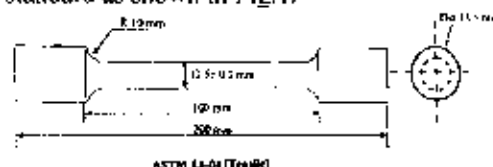


Figure 1 Dimensions of the tension test specimen.

The engineering stress on the bar is equal to the average uniaxial tensile force on the bar divided by the original cross-section area of bar.

$$\sigma = \frac{F}{A} \quad (1)$$

Where σ is Engineering stress (Mpa).
F is average uniaxial tensile force (N).
A is original cross-sectional (m^2).

2. Elongation is inversely proportional to tensile strength and hardness. The amount of elongation is expressed as a percentage of the original gauge length. Given by

$$\text{Percentage elongation} = \frac{L - L_0}{L_0} \times 100$$

where L is final gauge length.
 L_0 is original gauge length.

3. The Rockwell test is used to determine the hardness by measuring the depth of penetration of an indenter under a large load compared to the penetration made by a preload.

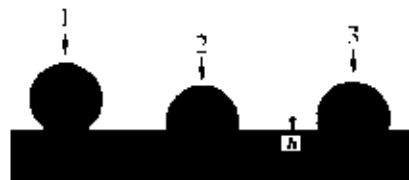


Figure 2 The steps in measurement of hardness with a sphere of steel.

$$\text{Rockwell B number} = \frac{130 - \text{depth of indentation}}{0.002}$$

Conduction heat transfer is the normal transfer of energy within solids. Conduction heat transfer also occurs through gases and liquids, but it then only predominates if the gases or liquids are stagnant or move slowly.

The mathematical model for conduction heat transfer is Fourier's Law of conduction,

$$\dot{Q}_x = -\kappa A \frac{\partial T}{\partial x} \quad (4)$$

where \dot{Q}_x is the heat transfer in the x direction the normal area A due to the temperature gradient $\partial T / \partial x$. The thermal conductivity κ is an index of ability of a material to conduct heat due to a temperature gradient in that material.

4. Research Outcome

4.1 Tensile test results

Tensile tests were performed on the gray cast iron specimens. Table 1 shows the tensile test results of three specimens made of 0.7, 1.5, and 2.8 inch mold wall thickness. As shown in Table 1, the results revealed that the tensile properties of the gray cast iron improved due to low cooling rates. The maximum of tensile strength, hardness and percentage elongation were 255.06 MPa, 210 Brinell and 0.82% of specimens with 1.5 inches mold wall thickness. The heat transfer of specimens casted with 0.7 inches mold wall thickness is 501.66 watts greater than that of 1.5 and 2.8 inch mold wall thickness.

The plots of the cooling rate curves as a function of time are shown in Fig.3. Constant temperature ranges are 668 °C, 680 °C, and 719 °C for 1.5, 0.7 and 2.8 inch mold wall thickness, respectively.

Table 1 mechanical testing.

Size	Tensile strength (MPa)	Elongation At break (%)	HB (Brinell)	Q _v (W)
0.7 inches	243.92	0.71	210	501.66
1.5 inches	255.06	0.82	210	476.57
2.8 inches	253.31	0.80	205	453.65

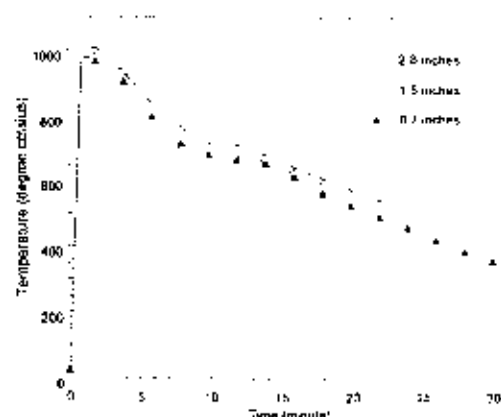


Figure 3 The plots of the cooling rate curves of the different mold wall thickness obtained

4.2 Microstructure

The XRD patterns of the specimens were shown in Fig xx. The XRD patterns show a single phase of cubic $Im\bar{3}m$ space groups. The data analysis reveals that the lattice parameter of the specimens is 2.86 Å. The optical emission spectroscopy test shows that the specimens are composted of Fe 93.17%, C 3.14 %, Si 2.65 %, and others.

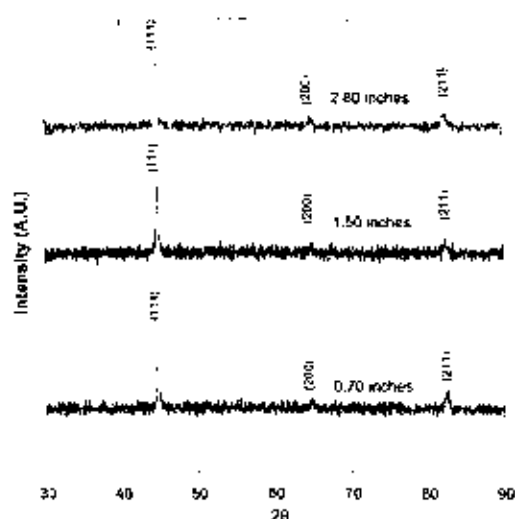


Figure 4 XRD pattern of the gray cast iron specimen.

The graphite flakes of the specimens were observed using an optical microscope after polishing and etching as shown in Fig.5 (A, B, C). The large graphite flakes seriously interrupt the continuity of the pearlitic matrix, thus reducing the strength and ductility of the gray iron. The small graphite flakes are less damaging and therefore generally preferred. Flake graphite is subdivided into five types (patterns), which are designated by the letters A through E. Fig.5 (A, B, C) graphite flakes present in type A. The orientation distribution of Type A graphite is random. It is the commonly preferred type of graphite giving optimum strength properties.

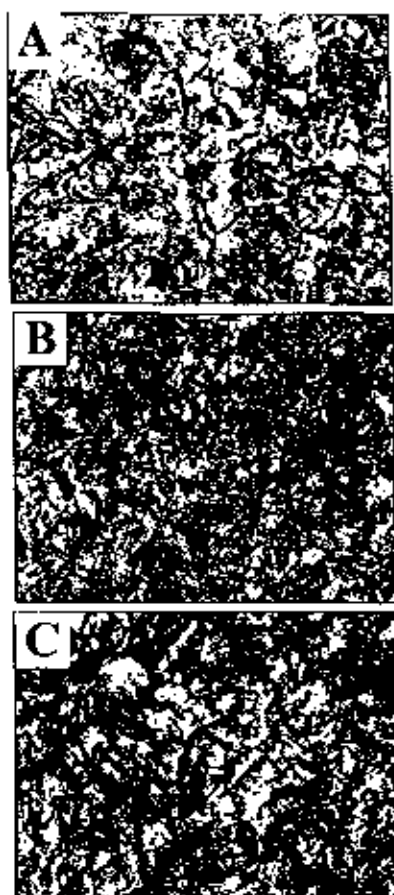


Figure 5 Microstructure (A) 0.7 inch (B) 1.5 inch and (C) 2.8 inch.

4.3 SEM observation

Figs. 6, 7 and 8 show the tensile fracture surfaces of the gray cast iron specimens. Fig. 6 (b) shows the fracture surface of the gray cast iron similar to flowers. The dendrite in metallurgy is a characteristic tree-like structure of crystals growing as molten metal freezes, as shown in Fig. 6 (A) produced by fast growth along energetically favorable crystallographic directions. This dendrite growth has large consequences in regards to material properties.

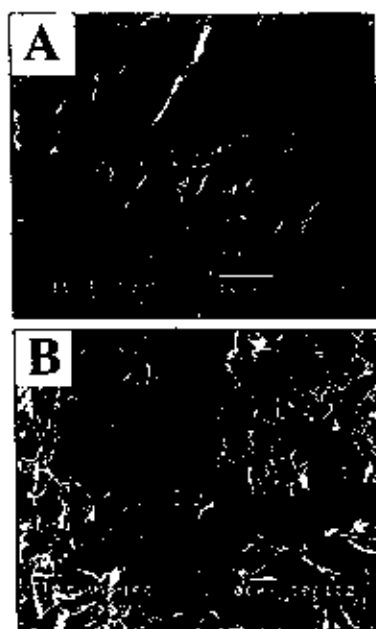


Figure 6 Tensile fracture surfaces of the mold wall thickness of 0.7 inches.

The main part of the fracture surface is the boundary between the graphite and metal matrix. Fig 6 and 7 show the fracture surface of graphite. The total elongation of the gray cast iron is about 0.71-0.80 %. The low value of total elongation yields a result in low tensile strength that causes low ductility and brittle.





Figure 7 Tensile fracture surfaces of the mold wall thickness of 1.5 inches.

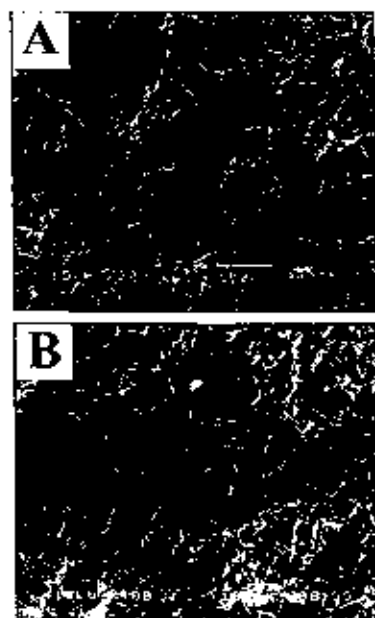


Figure 8 Tensile fracture surfaces of the mold wall thickness of 2.8 inches.

5. Discussion

The evaluation of the gray cast iron with different cooling conditions (the mold wall thickness of 0.7, 1.5, and 2.8 inch) shows that the cooling rate has an effect on the tensile properties, microstructure and hardness brinell (HB). All specimens are single phase of iron with cubic 1m-3m space group. The results of this work indicates that the tensile properties and hardness of the gray cast iron optimize when the mold wall thickness of 1.5 inches were casted.

The tensile fracture of the specimens made with the mold wall thickness of 0.7 inches has dendrite structure produced by fast cooling rate. This dendritic growth has large that results in low tensile strength.

6. Acknowledgement

We would like to thank Asst. Prof. Suriya Choksawadee and Dr.Charuayporn Santhaweesuk, Department of Industrial Engineering, Ubonratchathani University for valuable advices and sample preparation. We also thank Dr.Greg Heness, Department of Physics and advanced materials, University of Technology Sydney, for teaching and helping us with sample characterization and suggestion.

6. References

1. Collini, G. Nicoletto a. R. Konecna. (2008). Microstructure and mechanical properties of pearlitic gray cast iron. *Mater.Sci. Eng. A*, 488: 529-539.
- J.R. Davis. (1985). *Metallography and Microstructures*. ASM Metals Hand Book, vol. 9: 127-135.
- B.A Ceccarelli, R.C Dommarco, R.A Martínez, M.R MartínezGamba. 2004. Abrasion and impact properties of partially chilled ductile iron. *Wear*. Vol. 256: 49-55.
- J.V. Giacchi, R.A. Martínez, M.R. MartínezGamba, R.C. Dommarco. 2007. Abrasion and impact properties of partially chilled gray iron. *Wear*. Vol. 262: 282-291.
- Aver. Sidney H. (1987). *Introduction to Physical Metallurgy*. 2nd Ed. New York: McGraw-Hill.
- Kurt C. Rolle. (2000). *Heat and Mass Transfer*. New Jersey: Prentice-Hall.

The 4th UBRU International Research Conference.
An Integration of ASEAN Local Wisdom to International.

S. L. Kakani and Amit Kakani. (2004).
Material Science. New Delhi: New
Age International Publishers.

GanwarichPluphrach. (2010). Study of the
effect of solidification on graphite
flakes microstructure and mechanical
properties of an ASTM a-48 gray
cast iron using steel molds.
Songklanakarin J. Sci. Technol. 32
(6): 613-618.

GanwarichPluphrach. (2010). Study of the
effect of solidification on graphite
flakes microstructure and mechanical
properties of an ASTM a-48 gray
cast iron using steel molds.
Songklanakarin J. Sci. Technol. 32
(6): 613-618.



มหาวิทยาลัยขอนแก่น
๕๐ ปีแห่งการอุทิศเพื่อสังคม

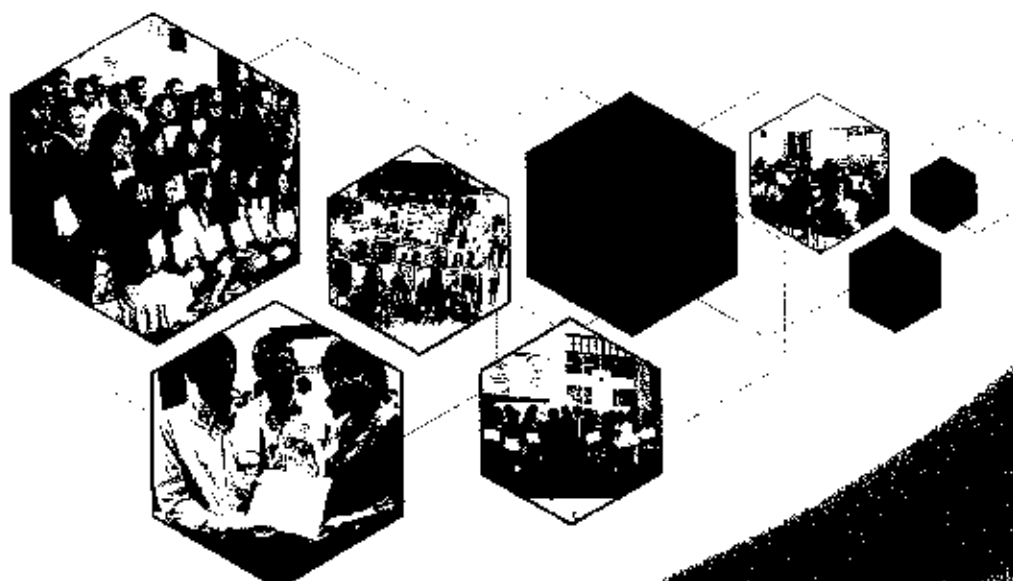
50 ปี มข. ถิ่นการอุทิศเพื่อสังคม

รวมบทคัดย่อ

การประชุมวิชาการเสนอผลงานวิจัย
ระดับบัณฑิตศึกษา ครั้งที่ 15

วันศุกร์ที่ 28 มีนาคม 2557

ณ วิทยาลัยการปกครองท้องถิ่น มหาวิทยาลัยขอนแก่น



บัณฑิตวิทยาลัย มหาวิทยาลัยขอนแก่น
GRADUATE SCHOOL MAHACHULALONGKORAJAVIDYALAYA UNIVERSITY



PMP1

การออกแบบและควบคุมอัตราการเย็นตัวเพื่อเพิ่มสมบัติความต้านทานแรงดึงของเหล็กหล่อ

Kiatkhun Sawasuk (กิตติคุณ เสาวสุก)* Dr. Udon Jeyaratch ๑๑.๐๐๑-๖๖๖๖๖๖**

ABSTRACT

The quality of cast iron was enhanced by controlling the cooling rate of cast iron in the manufacturing process. We have designed the gray cast iron process by modifying the thickness of a sand mold to get the proper tensile stress of the cast iron with regular structure. The mold was a cylindrical shape and made of sand. The process of heat transfer of the materials was investigated. The heat transfer rate was considered as the radial thickness of the mold wall. Three gray cast irons with the mold wall thickness of 0.7, 1.5, and 2.8 inches were casted and tested for tensile strength. The results show that the specimen made of 1.5 inch radial mold thickness yields the highest tensile strength.

บทคัดย่อ

[illegible]

Key Words: Cooling rate, Tensile strength, Gray cast iron

คำสำคัญ: จักรวรรดิโรมัน, ความสัมพันธ์ทางวัฒนธรรม, การตั้งถิ่นฐาน

* Student, Master of Science Program in Physics, Faculty of Science, Umm Al-Qadisiyah University

** Assoc. Prof. Department of Physical Sciences, Faculty of Science, Umm Al-Qadisiyah University

